AMERICAN UNIVERSITY OF BEIRUT

MODIFIED ELECTROSPUN TCH-TSC PVC MEMBRANES FOR THE REMOVAL OF HEAVY METAL IONS FROM WATER

by
BAHAA ALI CHAMMOUT

A thesis
submitted in partial fulfillment of the requirements
for the degree of Master of Engineering
to the Department of Civil and Environmental Engineering
of the Maroun Semaan Faculty of Engineering and Architecture
at the American University of Beirut

Beirut, Lebanon
August 2022

AMERICAN UNIVERSITY OF BEIRUT

MODIFIED ELECTROSPUN TCH-TSC PVC MEMBRANE FOR THE REMOVAL OF HEAVY METAL IONS FROM WATER

by

BAHAA ALI CHAMMOUT

Approved by:

Rana A. Bilbeisi Rana Bilbeisi Digitally signed by Rana Bilbeisi DN: cn=Rana Bilbeisi, o=AUB, ou=CEE, email=rb102@aub.edu.lb, c=LB Date: 2022.09.01 18:12:48 +03'00'

Dr. Rana Bilbeisi, Assistant Professor — Advisor
Department of Civil and Environmental Engineering

Ibrahim Alameddine Digital Signer:Ibrahim Alameddine DN:C=CA, E=ialameddine@gmail.com, CN=Ibrahim Alameddine Date:2022.09.01 09:02:33 -04:00

Dr. Ibrahim Alameddine, Associate Professor — Member of Committee
Department of Civil and Environmental Engineering

Ali Tehrani Digitally signed by Ali Tehrani DN: cn=Ali Tehrani, c=FI, o=Aalto University, ou=Bioproducts and Biosystems, email=ali.tehrani@aalto.fi Date: 2022.09.01 11:29:07 +03'00'

Dr. Ali Tehrani, Associate Professor — Member of Committee
Department of Bioproducts and Biosystems, Aalto University

Date of thesis defense: August 15, 2022

AMERICAN UNIVERSITY OF BEIRUT

THESIS RELEASE FORM

Student Name: __Chammout_____Bahaa_____Ali_____
Last First Middle

I authorize the American University of Beirut, to: (a) reproduce hard or electronic copies of my thesis; (b) include such copies in the archives and digital repositories of the University; and (c) make freely available such copies to third parties for research or educational purposes:

☒ As of the date of submission

☐ One year from the date of submission of my thesis.

☐ Two years from the date of submission of my thesis.

☐ Three years from the date of submission of my thesis.

Bahaa Chammout Digitally signed by Bahaa Chammout
DN: cn=Bahaa Chammout, o, ou, email=bac02@mail.aub.edu, c=LB
Date: 2022.09.01 10:37:35 -05'00'

01/09/2022

Signature Date

ACKNOWLEDGEMENTS

First and foremost, I would like to acknowledge my warmest thanks to my advisor Prof. Rana A. Bilbeisi, for her continuous support of my studies and research, for her incredible motivation and enthusiasm, and for her strong passion for science and continuous learning. Her advice was invaluable during the research and writing of this thesis, and I consider myself incredibly lucky to have had her as an adviser and mentor during my Master's studies.

I would also like to thank Prof. Ibrahim Alameddine and Prof. Ali Tehrani for serving on the committee of this study. Thank you for your motivation, discussions, and expert advice, which shaped and honed the quality of this study.

Aside from the committee, Prof. Bilbeisi's research group was always available in the lab for assistance, sharing their experience, and, most importantly, motivation and encouragement. Many thanks to Dr. Amani Jaafar for her laboratory help and support during the project, which was developed and launched based on her current and prior research. I would also want to thank Ms. Fatima Youness for her unwavering assistance in the lab. This study expands on Ms. Youness' prior research methods, which she enthusiastically instructed me on in order for me to carry out this research.

I would like to acknowledge the Environmental Engineering Research Center (EERC) and the K. Shair Central Research Science Laboratory (CRSL) at AUB for providing the required equipment to carry out this research work. I would like to namely thank the CRSL lab manager, Ms. Rania Chatila, for her laboratory training, constant laboratory support for the past year, and for her expert advice on handling the equipment.

Lastly, I would like to thank my family and friends for their unwavering support and for always putting a smile on my face whenever my research hit a rough patch. Their support was crucial for returning to the study, learning, and progressing, culminating in what is offered here today.

ABSTRACT
OF THE THESIS OF

Bahaa Ali Chammout for Master of Engineering
Major: Environmental and Water Resources Engineering

Title: Modified Electrospun TCH-TSC PVC Membrane for the Removal of Heavy Metal Ions from Water

Pollutants discharged into a water basin from natural and anthropogenic sources result in degrading the quality of water. Water pollution is not only one of the leading global risk factors for illness, disease, and mortality; but it also contributes to the ongoing loss of accessible potable water globally. Heavy metals, in particular, are a class of water pollutants with a negative impact on aquatic life, the benthic environment, and human health because of their non-biodegradability, bioaccumulation, and toxicity. The latter spurred the development of a variety of water treatment approaches, including adsorption, as efficient water treatment technology, its use was attributed to the simplicity, low cost of implementation, and potential for regeneration and reusability of the adsorbents; prompting a green and sustainable water treatment approach. Because of their morphological properties and functionalization potential, electrospun polymeric nanofibrous membranes are among the most efficient adsorbents used for water treatment.

In this study, polyvinyl chloride (PVC) membranes are electrospun and modified with thiocarbohydrazide (TCH) and thiosemicarbazide (TSC), which are organic ligands known to bind heavy metals and enhance metal adsorption on the surface of an adsorbent. This study focuses on the removal of silver(I), mercury(II), cadmium(II), and lead(II) ions from synthetic water using modified membranes. The complexation of TCH/TSC ligands to the studied metals was investigated using UV-visible spectroscopy. The complex (metal:ligand) formation, stoichiometry, and binding affinity were modeled using the Benesi-Hildebrand relationship for Ag(I) and Hg(II) ions. Electrospun and modified membranes (TCH/TSC-PVC membranes) were then characterized and evaluated for heavy metal removal. Modification of the surface of PVC membranes with TCH resulted in enhancing the removal of Ag(I) by 40% and Hg(II) by 70%, whereas the modification with TSC ligand resulted in an improved removal of Ag(I) by 97.5% and Hg(II) by 76.6% in 24 hours.

The adsorption parameters of TSC-PVC towards Ag(I) and Hg(II) and the recyclability of the membrane were investigated. The adsorption kinetics of the membranes were best fitted with the pseudo-second order model. The equilibrium data were strongly aligned using the Langmuir adsorption isotherm model, with maximum adsorption capacities of 62.1 mg/g for Ag(I) and 20.0 mg/g for Hg(II). TSC-PVC was also shown to exhibit strong selectivity for Ag(I) and Hg(II) ions in a mixed metal system including silver(I), mercury(II), cadmium(II), lead(II), copper(II), and zinc(II) ions. Additionally,

the TSC-PVC membrane was regenerated under mildly acidic conditions and demonstrated constant sorption effectiveness across three adsorption/desorption cycles.

Keywords

Adsorption, water treatment, electrospun-nanofibrous membrane, surface modification, heavy metals, metal-organic complexes, and sustainable water treatment technologies.

TABLE OF CONTENTS

ILLUSTRATIONS

Figure

TABLES

Table

CHAPTER I

INTRODUCTION

A. Water Pollution

Freshwater, which accounts for only 3% of the world's water, is naturally unequally distributed throughout the globe. Furthermore, only 0.9% of the world's freshwater (0.000027% of the world's water storage) is available for human use as surface water (rivers and lakes), with the remainder embedded in underground water tables or glaciers (Bralower & Bice, 2022). The distribution of water around the earth's surface is presented in Figure 1.

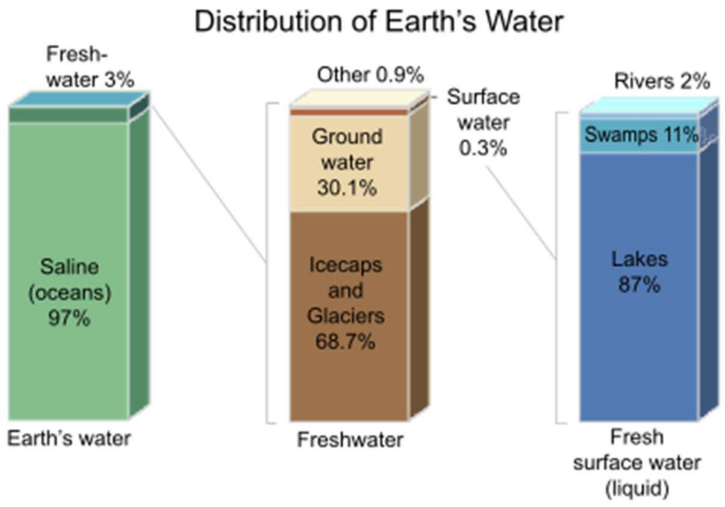

Figure 1. Distribution of earth's water (Bralower & Bice, 2022*)*

With global population growth, rapid urbanization, and economic and agricultural development, the burden on the scarce freshwater resources got exaggerated, spurring migration, conflicts, and worsening community socioeconomic well-being (Famiglietti, 2014). Water scarcity has affected over 1.6 billion people

worldwide as a result of unequal distribution and unbalanced use (Molden, 2013); it is expected to affect more than two-thirds of the world's population by 2025 (WWF, 2022).

Not only is freshwater scarce, but many freshwater resources, particularly those available as surface water, are contaminated. Anthropogenic activities, such as industrial and agricultural operations that discharge contaminated effluents into water basins, are the primary cause of water pollution; primarily surface water, which can also become contaminated through agricultural and industrial runoff, and subterranean freshwater tables, which are reached through effluent infiltration into the soil.

Furthermore, industrialization concentrated human activity in cities, resulting in undue overpopulation (Ariaratnam & Chammout, 2021). Because of the rapid change in land use/land cover, human activities now have a greater impact on the world's ecology, ecosystem, and hydrology (Ndulue et al., 2015). As cities expand, more surface area is covered with concrete, asphalt, and other construction materials. The latter transformed the soil into an impermeable surface, resulting in less infiltration and an increase in the rate and volume of runoff. Toxic contaminants are transferred with runoff to surface freshwater bodies and infiltrate into underground freshwater tables; significantly degrading water quality.

Water quality may be degraded by a variety of contaminants, namely organic and inorganic pollutants. Many organic pollutants undergo degradation in water due to microbial activities, diminishing dissolved oxygen and water quality. On the other hand, inorganic pollutants, particularly heavy metals, enter the aquatic food chain and their concentration gets amplified via the bioaccumulation process, as illustrated in Figure 2. Heavy metals are soluble in water, but unlike many other contaminants, they are non-

biodegradable, this leads to a higher propensity for bioaccumulation and reaches substantial toxicity levels at low concentrations. This causes significantly adverse impacts on ecosystems and human health (Zhuang et al., 2009; Gall et al., 2015; Liu et al., 2017).

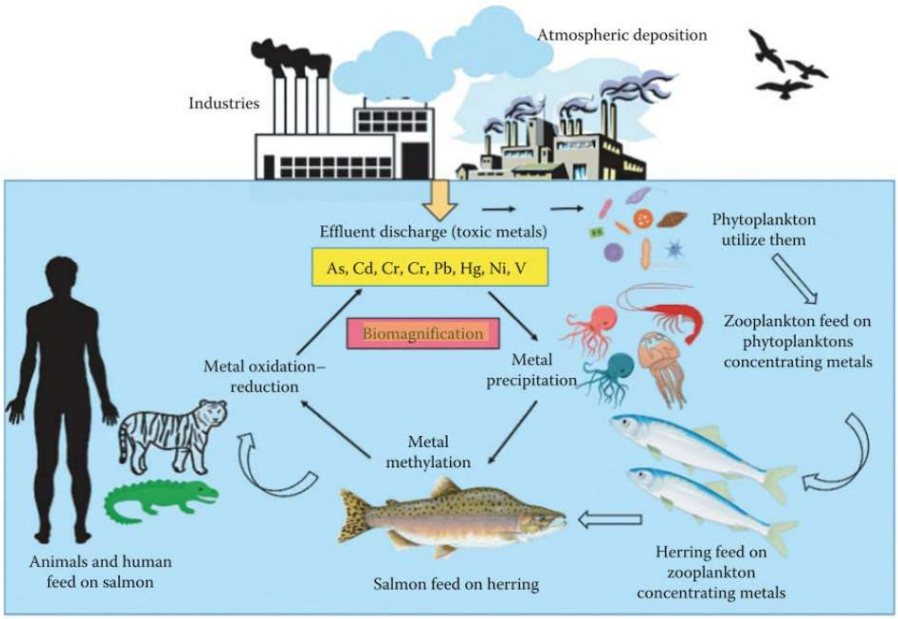

Figure 2. Bioaccumulation of heavy metals (Das and Dash, 2017)

Heavy metals are natural constituents of the earth, yet the rapid and dispersed anthropogenic activities have altered their geochemical cycles in the environment (Chang et al., 2019). Heavy metals have become widely utilized in a range of industries, including agriculture (He et al., 2019), manufacturing, and electronics (Tchounwou et al., 2012), contributing to a tremendous rise in human exposure to heavy metals.

Heavy metal concentrations bio-magnify throughout the bioaccumulation process, reaching individuals at dangerous levels through food or drinking water. This exposes individuals to chronic and sub-chronic diseases not limited to cancer, diabetes, and nervous system and heart problems (Tchounwou et al., 2012).

1. Lead

Lead is a heavy metal that occurs in two oxidation states: divalent (II) and tetravalent (IV). The most abundant form of lead in the environment is Pb(II), which exists in the form of salts that are soluble in water. Lead(IV), on the other hand, is a potent oxidizing agent that is rarely found on the Earth's surface (Sigel et al., 2017).

Lead(II) is widely used in industrial applications such as batteries, electronics, and metallurgy, with a global production of 10 million tons by 2012 (Sigel et al., 2017). Despite the versatility of its applications, exposure to lead(II) threatens human health; targeting the renal, reproductive, and neurological systems (Kim et al., 2012; Jarup, 2003; Liu et al., 2013; Wang et al., 2014).

Even with public knowledge of lead poisoning, it is nevertheless frequently detected in the ecosystem, namely water bodies, at alarming rates much beyond the permitted levels indicated in Table 1, establishing a problem that must be addressed.

2. Mercury

Mercury is a heavy metal that occurs in two oxidation states: monovalent (I) and divalent (II). Mercury is often found in the environment in the second oxidation state Hg(II), where it forms inorganic complexes such as mercuric oxide (HgO), which is used in mercury cell batteries (Baird & Cann, 2012).

Mercury is discharged from natural and anthropogenic sources. The former includes volcanic activity and the erosion of mercury-containing sediments, whereas the latter is primarily concerned with the burning of fossil fuels and the significant use of mercury in industry and agriculture (Figueiredo et al., 2017). Mercury's uses in research and industry span from laboratory items like barometers and thermometers to medicinal

products such as dental amalgams. Furthermore, mercury is utilized in agriculture as a foliar spray to combat plant diseases (Beckers & Rinklebe, 2017).

Mercury is one of the most toxic heavy metals in the environment owing to its volatility (Cheng et al., 2017). Mercury poisoning can have dire effects on the neurological system, kidneys, and liver (Beckers & Rinklebe, 2017).

In terms of water contamination, the majority of the mercury present in water is in the inorganic form Hg(II) and the organic form methylmercury $[CH_3Hg]^+$ (Beckers & Rinklebe, 2017). Methylmercury binds to the sulfhydryl group of proteins in fish, and undergoes a bioaccumulation process reaching the human body (Ritger et al., 2018). In the human body, and due to its lipophilic properties, methylmercury exhibits a half-life of 70 days (Baird & Cann, 2012), and causes serious health effects. This pollutant can cross the blood-brain barriers, making it the most hazardous form of mercury (Cesario et al., 2017).

3. Silver

Silver is a heavy metal that is most usually found in its monovalent (I) oxidation state, such as silver nitrate $AgNO_3$, with fewer occurrences of divalent (II) and trivalent (III) forms.

Almost every electrical equipment contains silver. The metal ion is a necessary coating material for electronic connections in automobiles. Silver's electric conductivity makes it an ideal metal for all electronics, including television screens, circuit boards, and even solar energy devices.

Silver has antibacterial characteristics and is employed as a water bacteriostat; nevertheless, if consumed at quantities higher than those listed in Table 1, it may

produce argyria; a skin discoloration (RSC, 2022). Furthermore, large levels of soluble silver can induce liver and kidney damage, as well as eye, skin, intestinal, and respiratory irritation (Drake & Hazelwood, 2005).

4. Cadmium

Cadmium is a heavy metal that is mainly found in the divalent form (II), with the monovalent oxidation state (I) occurring infrequently.

Cadmium is a very toxic heavy metal that is widely utilized as a raw material in nickel-cadmium batteries, as well as in various electrical applications and paint pigments (Buxbaum & Pfaff, 2005). Cadmium products nearly doubled twenty-five times in the last decade, as seen in Figure 3.

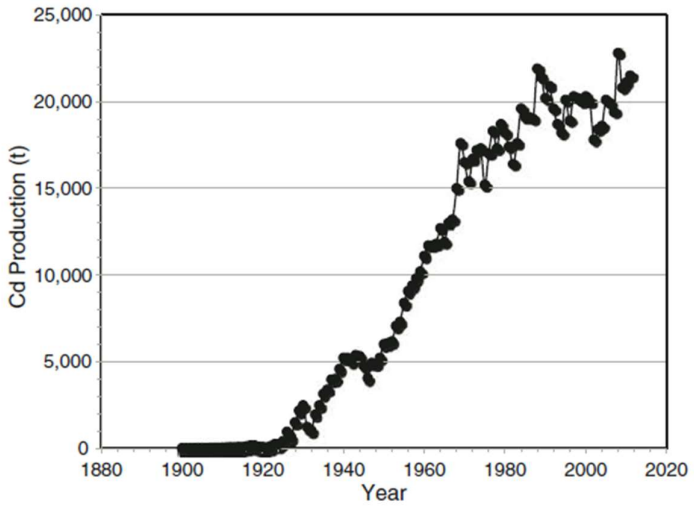

Figure 3. World production of cadmium metal (U.S. Geological Survey, 2012)

Cadmium is very hazardous to all living things. Waste batteries wound up in landfills due to increased manufacturing and inadequate recycling of nickel-cadmium batteries, potentially affecting subsurface water through leaching. Furthermore, various industrial and mining operations discharge cadmium into bodies of water (Rahimzadeh

et al., 2017). Even at low doses, cadmium binds to the mitochondria, limiting cellular respiration and oxidative phosphorylation (Patrick, 2003). Cadmium then produces organ system toxicity, including reproductive, cardiovascular, neurological, and respiratory system toxicity. Furthermore, long-term cadmium exposure may cause several forms of cancer (Rahimzadeh et al., 2017).

B. Water Treatment Approaches

Heavy metals' negative effects on human health and the environment necessitated the establishment of worldwide regulations by the World Health Organization (WHO) and the Environmental Protection Agency (EPA) to restrict the permitted exposure to heavy metals in drinking water. The worldwide drinking water regulations for some of the most common heavy metals in water are shown in Table 1.

Table 1. International drinking water standards for heavy metals

Heavy metal	**International Allowable Standards (mg/l)**	
	WHO (2011)	**EPA (2012)**
Arsenic	0.01	0.1
Cadmium	0.003	0.005
Chromium	0.05	0.1
Copper	2	1.3
Lead	0.01	0.015
Mercury	0.006	0.002
Silver	0.1	0.1

Degraded water quality is a key environmental hazard that threatens the well-being of human populations and wildlife, hence, the search for sustainable water treatment technologies is an active research area.

Heavy metal pollution, in particular, poses serious risks to human health and the environment whether from natural sources or, more typically, anthropogenic industrial operations. Heavy metals require extensive removal treatment from water resources in order for their concentrations to reach acceptable levels. Numerous wastewater treatment (WWT) processes have been developed to reduce heavy metals, including chemical precipitation, coagulation and flocculation, ion exchange, membrane exchange, and electro-dialysis. However, the majority of these systems are constrained by high operational and maintenance costs, limited treatment efficiencies, and the generation of secondary pollutants; especially toxic sludge (Bhatnagar et al., 2015).

Adsorption, on the other hand, is a preferable treatment option due to its ease of design and operation (Ali et al., 2012; Gautam et al., 2014; Bhatnagar et al., 2015). Furthermore, adsorption techniques offer a relatively high capacity for pollution removal and broader applicability (Siyal et al., 2018). Notably, adsorbents could potentially be regenerated and effectively reused, which is an important quality in green and sustainable water treatment systems.

Adsorption is the process by which a solute in a solution is drawn to the surface of a solid adsorbent and sequestered by the adsorbent due to physical or chemical interactions (Gao et al., 2013; Crawford & Quinn, 2017). In wastewater treatment, activated carbon adsorption is often used to sequester the residues of biological and chemical oxidation, such as heavy metals (Lofrano, 2012; Tchobanoglous et al., 2003). However, the use of activated carbon is restricted due to the relatively high treatment costs (Gautam et al., 2014) and the low regeneration capability (Feo & Gisi, 2014).

Low-cost adsorbents derived mostly from agricultural and industrial materials have been developed to replace activated carbon in heavy metals sequestration. By-

product adsorbents are environmentally favorable since they decrease by-product disposal, and can reduce wastewater contamination at reduced costs (De Gisi et al., 2016). However, the removal efficiency of these low-cost adsorbents is often restricted, as is the requirement for certain environmental conditions such as pH and temperature (De Gisi et al., 2016).

Based on the foregoing, there is a need for the development of highly efficient and low-cost adsorbents that can be recycled or disposed of in an ecologically friendly manner.

Adsorption has been successfully used as an efficient approach for removing heavy metals from water. This is owing to the relatively high removal efficiency/capacity, low cost, flexible synthesis and operations, and the possibility of regenerating adsorbents and recycling them in water treatment cycles.

Electrospun membranes are among the emergent technologies in adsorption, as the polymeric nanofibers can be synthesized in a very short period of time, and have numerous applications in water filtration, nanotechnology, and biotechnology (Feng et al., 2013). Polymeric electrospun membranes have been studied in recent years for their ability to adsorb heavy metals from water (Suja et al., 2017; Zhu et al., 2021). Nanofibrous membranes are highly porous and may be surface modified by functional groups to improve adsorption efficiencies, making them ideal candidates for pollutant sequestration from aqueous solutions. Current investigations on functionalized nanofibrous membranes for heavy metal sequestration, as well as the removal capacities attained, are summarized in Table 2.

Table 2. Review articles on modified electrospun membranes for the removal of heavy metals

Polymer	Functional Group	Heavy Metal	Adsorption Capacity/Removal Efficiency	Reference
Polyethyleneimine (PEI) cross-linked P84	Poly (acrylic acid-co-maleic acid) (PAM), poly (acrylic acid) (PAA), and poly (dimethylamine-co-epichlorohydrin-co-ethylenediamine) (PDMED)	Cr, Zn, Ni, Cu, Cd, and Pb	> 97%	Gao et al. (2014)
Polyacrylonitrile (PAN)/polyaniline (PANI)-nylon	Diethylenetriamine (DETA)	Pb(II)	960 mg/g	Almasian et al. (2018)
		Cd(II)	911.72 mg/g	
Polyacrylonitrile/cellulose acetate (PAN/CA)	Hydrolysis and amidoximation	Fe(III)	7.47 mmol/g	Feng et al. (2018)
		Cu(II)	4.26 mmol/g	
		Cd(II)	1.13 mmol/g	
Chitosan/Polyvinyl alcohol (PVA)/ polyether sulfone (PES)	Fe_3O_4 nanoparticles	Cr(IV)	509.7 mg/g	Koushkbaghi et al. (2018)
		Pb(II)	525.8 mg/g	
Cellulose	Citric acid	Cu(II)	399.14 mg/g	Zang et al. (2018)
Chitosan/poly (glycidyl methacrylate) (PGMA)/polyethyleneimine (PEI)	Amino group	Cr(VI)	138.96 mg/g	Yang et al. (2019)
		Cu(II)	69.27 mg/g	
		Co(II)	68.31 mg/g	

Polymer	Functional Group	Heavy Metal	Adsorption Capacity/Removal Efficiency	Reference
Poly methacrylic acid (PMA)/Cellulose acetate	-	Pb(II)	146.2 mg/g	Zang et al. (2019)
Polyvinyl alcohol (PVA) and polyacrylic acid (PAA)	Thiol-modified silica nanoparticles	Cu(II)	125.47 mg/g	Kim et al. (2019)
Polyvinyl chloride (PVC)	Thiol-functionalized HMO nanoparticles	Cu(II)	90%	Hezarjaribi et al. (2020)
		Ni(II)	90%	
Polyvinyl chloride (PVC)	Triethylenetetramine	Pb(II)	1250 mg/L	Youness (2021)

Various treatment methods have been developed and evaluated for the removal of heavy metals. Chemical precipitation, ion exchange, and membrane filtration have been studied for the removal of Pb(II) (Fu & Wang, 2011; Zhao & He, 2014), with generally limited efficiencies.

Significant efforts have been made to remove Hg(II) from the environment, including the use of diverse technologies such as hydrogels, porous silica, metal particles, metals organic frameworks (MOFs), and covalent organic frameworks (COFs), all of which have shown potential success in the removal of Hg ions from water (Cheng et al., 2017).

Silver, which may be employed as a bacteriostat, should be kept to acceptable levels. Reverse osmosis, distillation, and cation exchange can all be used to extract silver ions from water (WQA, 2004). Although these traditional technologies yield significant silver removal; they are inherently energy demanding.

Cadmium, an acute toxin, has been studied for purification from water sources primarily by biological activity, namely phytoremediation and phytochelation

(Haribabu & Sudha, 2011). Although natural chelation has the ability to remove cadmium, it takes significantly longer time than chemical adsorptions, potentially necessitating months. Furthermore, heavy metal ions are adsorbed on plant cell tissue during phytoremediation; necessitating further treatment of plant waste biomass to minimize secondary contamination/human exposure.

Based on the aforementioned removal technologies and their relative limitations, this study investigates the development of two novel adsorbents based on the modification of electrospun PVC membranes with organic ligands. PVC membranes will be electrospun according to an established protocol before being modified with the organic ligands, thiocarbohydrazide (TCH) and thiosemicarbazide (TSC). Adsorption parameters and removal effectiveness of TCH/TSC modified PVC membranes against the four heavy metal contaminants will be examined.

C. Organic Ligand as Modification Agents

Metal chelation proceeds through the formation of coordination (non-covalent) bonds between organic ligands and metal ions resulting in a metal-organic complex. This interaction can be exploited for the removal of heavy metals from water, especially if the organic ligand is suspended on a solid support. Organic ligands interact with metal ions based on their functionalities, those with oxygen and nitrogen as donor atoms have received the greatest attention due to their strong interaction with metal ions. Yet, the interest in sulfur donor chelating agents has expanded over the years, and the number of chemical investigations in this field has increased significantly (Ali & Livingstone, 1974).

Thiosemicarbazones (TSCs) and their derivatives, having the general formula of $R^1R^2C{=}N{-}NH{-}C(=S){-}NR^3R^4$, are composed of sulfur and nitrogen donor groups capable of interacting with metal ions in solution, forming metal-organic complexes (Prajapati & Patel, 2019), as depicted in Figure 4. These complexes have been mostly reported for antifungal and antibacterial activities (Jaafar et al., 2020), with few reports on their water treatment applications (Jaafar et al., 2021).

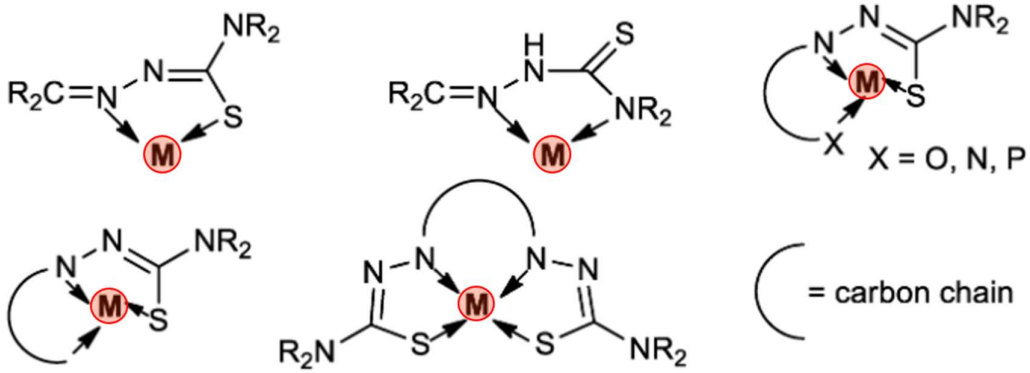

Figure 4. Metal coordination by TSCs ligands (Kostas & Steele, 2020)

1. Thiocarbohydrazide (TCH)

Thiocarbohydrazide, also known as carbonothioic dihydrazide, dihydrochloride, and dihydrate is a functional group containing sulfur and nitrogen, their structural formula is presented in Figure 5. The organic polyamine molecule's properties of metal-binding were explored in biological applications for therapeutic usage (Metwally et al., 2012). Abu-Hussen and Emara (2004) examined the complexation of thiocarbohydrazide (TCH)-based ligands with heavy metals such as Cr(II), Fe(III), Co(II), Ni(II), and Cu(II) for antibacterial activities.

For metal ion binding, thiocarbohydrazide, with the formula N^1H_2-N^2H-C(=S)-N^3H-N^4H_2, has two nitrogen donor atoms, which are the terminal ones N^1 and N^4, and the sulfur donor atom in most cases (Bacchi et al., 1999; Emara et al., 1995).

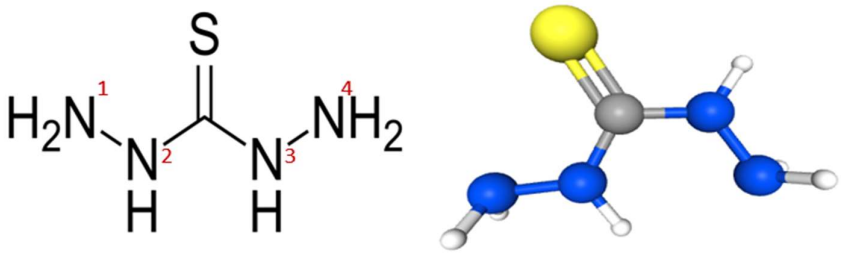

Figure 5. Structure of the thiocarbohydrazide (National Center for Biotechnology Information, 2022)

As TCH is a safe ligand utilized in biological activities, this organic ligand will be employed in physicochemical water treatment applications; by modifying the surface of a PVC membrane to be subsequently used to sequester heavy metals. The chemical modification/functionalization process involves the substitution of a chlorine atom in the PVC membrane with the terminal NH_2 (Moulay, 2010). This, potentially, leaves one terminal nitrogen and the sulfur capable of donating electrons to metal ions, creating coordination bonds and, as a result, allow for metal sorption from solution, as depicted in Figure 6. Other potentially occurring binding motifs are also presented.

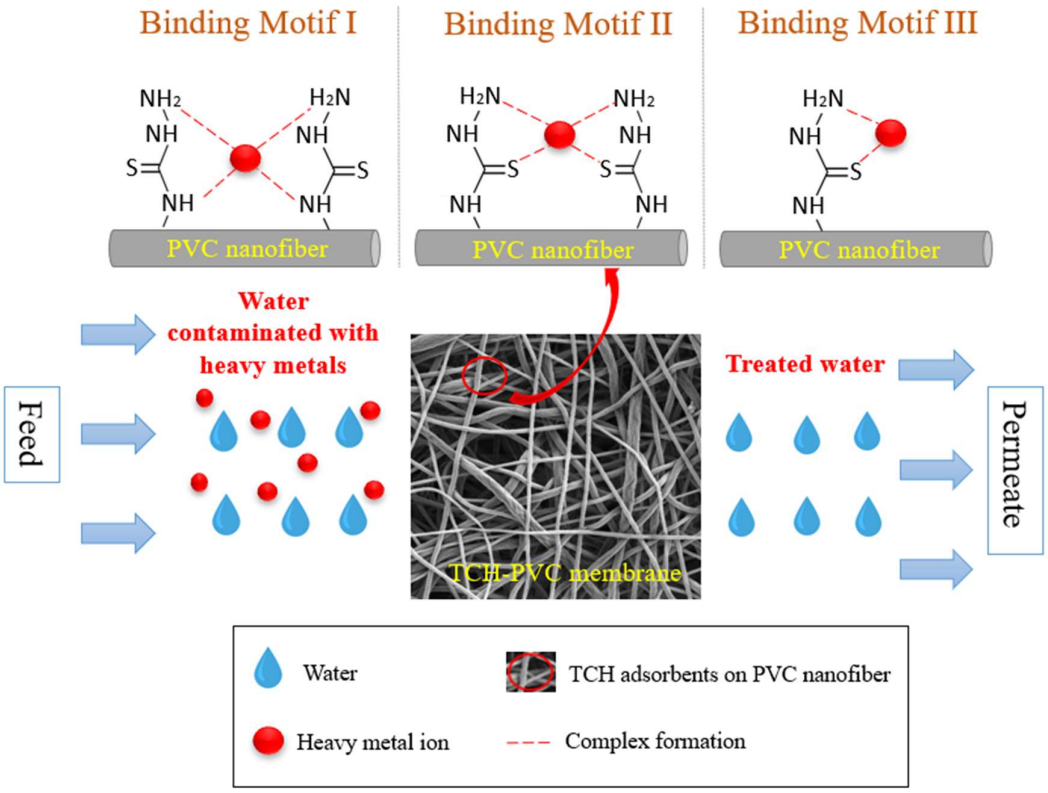

Figure 6. Proposed schematic representation of TCH-PVC membrane and metal coordination by TCH ligand

2. Thiosemicarbazide (TSC)

Thiosemicarbazide, also known as hydrazinecarbothioamide, and N-aminothiourea is a functional group containing sulfur and nitrogen, their structural formula is presented in Figure 7.

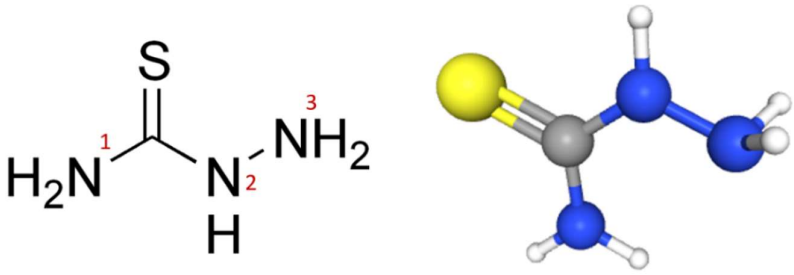

Figure 7. Structure of the thiosemicarbazide (National Center for Biotechnology Information, 2022)

TSC-based derivatives have been developed for heavy metal removal. Thiosemicarbazide modified chitosan showed significant removal of Pb(II) and Cd(II) ions from water (Li et al., 2016), and TSC-functionalized MOFs were observed for mercury removal from water with a sorption efficiency of 97% in two hours (Jaafar et al., 2021). Accordingly, and as TSC is a safe ligand and known metal chelator, this organic ligand will be employed in physicochemical water treatment applications; by functionalizing the surface of a PVC membrane to be subsequently used to sequester heavy metals. The chemical modification process involves the substitution of a chlorine atom in the PVC membrane by the terminal NH_2. This leaves primarily the sulfur able to donate electrons to create coordination bonds, as shown in binding motif II in Figure 8, and subsequently, achieve metal chelation. Based on changes in nucleophilicity during metal-ligand interaction, the secondary nitrogen might potentially donate electrons, and hence additional probable binding motifs are also presented. Furthermore, a combination of binding motifs I & II is highly probable in the octahedral metal complexation, such as mercury-TSC chelation, which is investigated in this study.

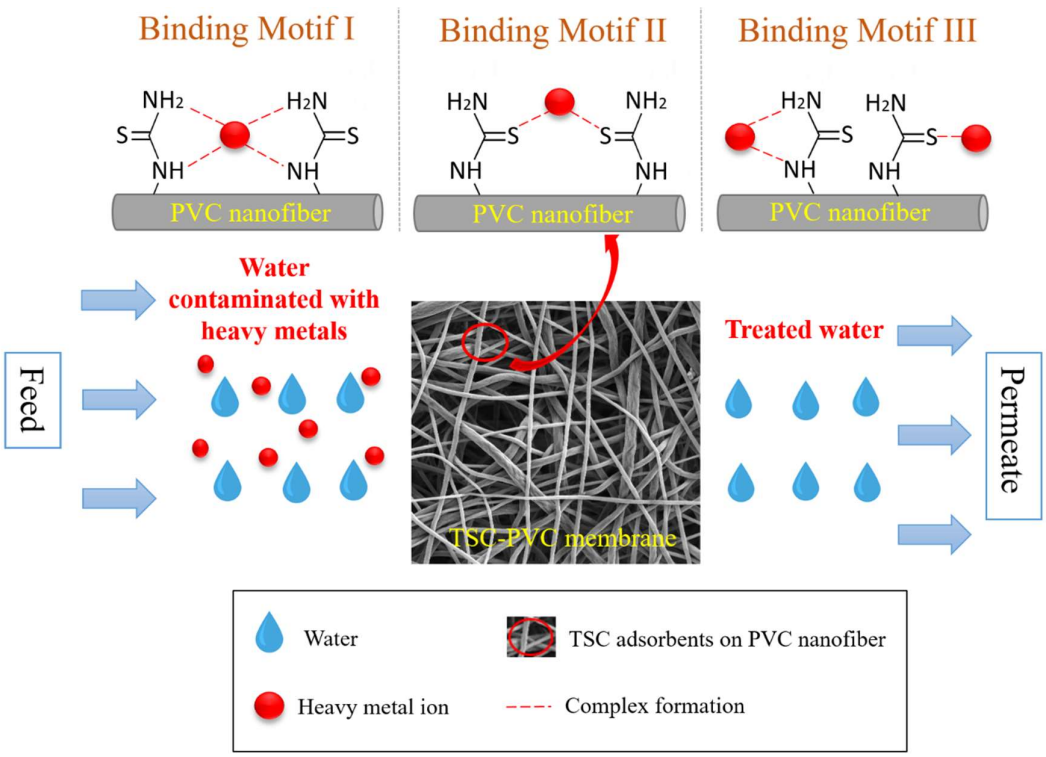

Figure 8. Proposed schematic representation of TSC-PVC membrane and metal coordination by TSC ligand

CHAPTER II

RESEARCH OBJECTIVES

Degraded water quality is a key environmental hazard that threatens the well-being of human populations and wildlife, hence, the search for sustainable water treatment technologies is an active research area. Owing to its sorption capacity, flexible synthesis and operations, relatively low cost, and ability to regenerate, adsorption has been investigated and employed as an effective method for the removal of heavy metals from water.

This work intends to build on the previous results of heavy metals removal utilizing modified electrospun membrane adsorbents, by developing functionalized electrospun membranes and investigating their potential for sequestering heavy metals from water. In this study, polyvinyl chloride (PVC) is the polymer used to prepare the membranes due to its morphological features including high surface area as well as the potential for modification. The surface of the PVC membranes is modified with two organic ligands; thiocarbohydrazide (TCH)/thiosemicarbazide (TSC). Both ligands are known to chelate metals in solution with a relatively high affinity. This study aims to expand on the application of TCH/TSC-metal complexation, which was mainly analyzed for anti-bacterial activities, by investigating their applicability in water treatment systems. The metal adsorption properties of the ligands will be evaluated after they have been utilized as modification agents of electrospun PVC nanofibers, which will be subsequently used for the removal of heavy metals from water, with a focus on lead(II), mercury(II), silver(I), and cadmium(II) ions. The steps followed to achieve the objectives of this are illustrated in Figure 9.

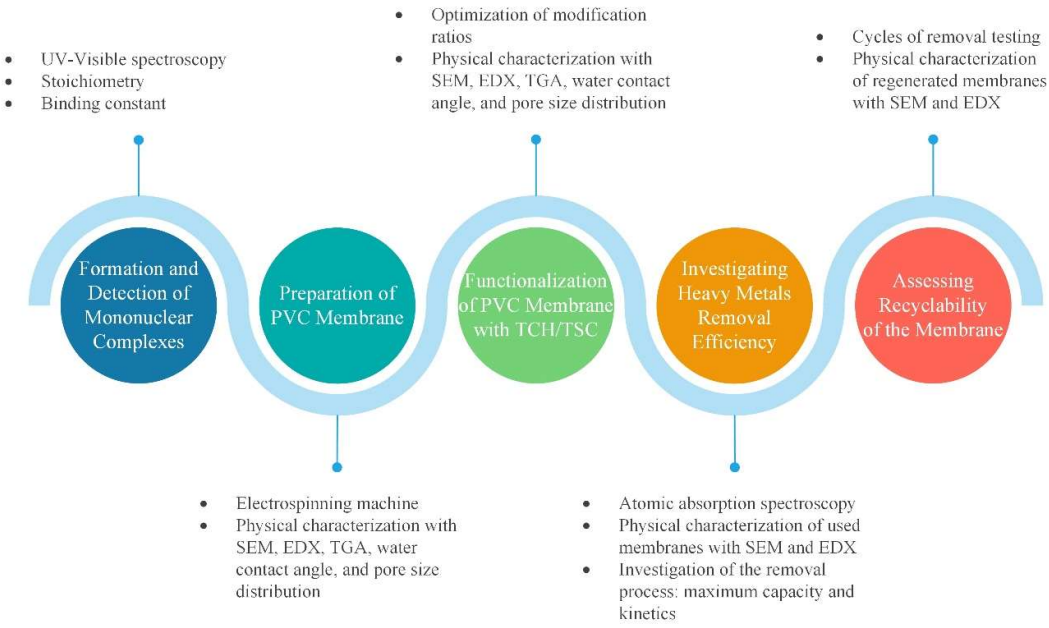

Figure 9. Steps to achieve research objectives

CHAPTER III

METHODOLOGY

The laboratory research was carried out in five phases, as outlined in Figure 9:

I- Detection of the selected heavy metals-TCH/TSC complexes in solution.

II- Fabrication of the electrospun PVC membranes.

III- Chemical modification/functionalization of the fabricated PVC membranes with TCH and TSC ligands, followed by the characterization of the functionalized nanofibers.

IV- Investigation of the metal removal properties of TCH/TSC-PVC membranes.

V- Regeneration of the modified membranes for reuse in numerous metal removal cycles.

Chemicals and laboratory equipment were employed for each of these processes. First, UV-visible spectroscopy was used to characterize and monitor the formation of heavy metal-TCH/TSC complexes. An electrospinning machine was utilized to fabricate the PVC membrane, which was subsequently chemically modified and physically characterized by scanning electron spectroscopy, energy dispersive X-ray, water contact angle, pore size distribution, and thermogravimetric analysis. Following the membrane functionalization and water treatment trials, the removal effectiveness was assessed using atomic absorption spectroscopy.

A. Materials

For heavy metals solutions, iron(II) trifluoromethanesulfonate ($C_2F_6FeO_6S_2$) with a molecular weight of 353.98 g/mol, lead(II) acetate trihydrate ($Pb(OAC)_2$) with a

molecular weight of 379.33 g/mol, mercury(II) trifluoroacetate ($C_4F_6HgO_4$) with a molecular weight of 426.62 g/mol, silver(I) nitrate ($AgNO_3$) with a molecular weight of 169.87 g/mol, and cadmium(II) nitrate ($Cd(NO_3)2.5H_2O$) with a molecular weight of 308.49 g/mol were all purchased from Sigma Aldrich.

The electrospun membranes were prepared using commercially available PVC with a molecular weight of 80,000 g/mol and a density of 1.4 g/mL, dimethylformamide (DMF), and tetrahydrofuran (THF) with 99.8% purity respectively. Furthermore, during the membrane fabrication, a commercial nylon screen fabric with an average pore size diameter of 350 μm and thickness of 215±2 μm was employed to support the membrane on the rotating drum.

B. UV-Visible Spectrophotometer

An Agilent 8453 UV-visible (UV-Vis) spectrophotometer was used to characterize and monitor the formation of the metal-ligand complexes. The UV-Vis is shown in Figure 10 below. Samples were sequentially placed in a normal quartz cuvette and the transparent cuvette was then placed in the apparatus for analysis. Following Beer's Law, the quantity of light absorbed by the sample is a surrogate assessment of its concentration in solution, and it is measured against the wavelength.

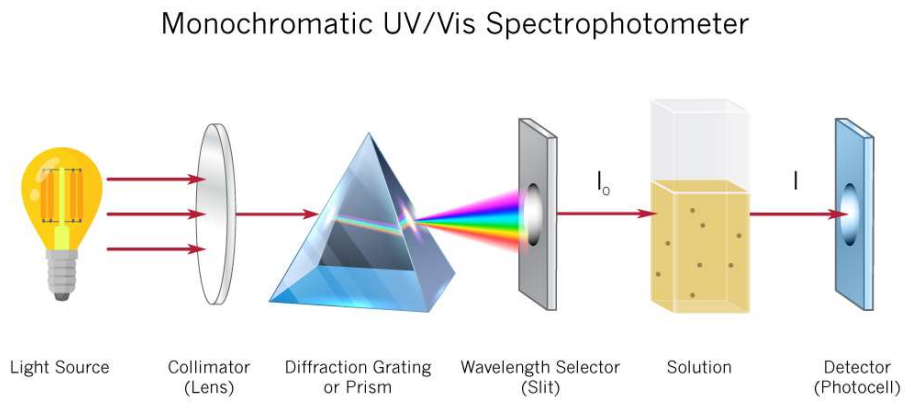

Figure 10. Schematic diagram of the optical setup of UV-visible Spectrophotometer (Implen, 2021)

To validate the complex formation, UV-Vis spectroscopy was used throughout the titration of TCH/TSC solutions with synthetic solutions rich in iron(II), lead(II), mercury(II), silver(I), or cadmium(II) ions. This was accomplished by titrating a TCH/TSC aqueous solution with an incremental concentration of heavy metals and analyzing the samples' absorption spectra in the 190-1100 nm region. The latter was used to validate the interaction of heavy metal ions with the TCH/TSC ligands in water. UV measurements were recorded at each titration increment during testing at room temperature and neutral pH. UV-Vis spectroscopy was used to investigate the binding and stoichiometry of metal-organic ligand complexes of varied ratios.

C. Electrospinning Machine

Electrospinning is a membrane fabrication approach used for the preparation of porous nanofibrous polymeric membranes with a high volume-to-surface area ratio. Notably and pertinent to this work, these nanofibrous membranes are flexible, allowing

them to be modified/functionalized with organic ligands to serve in various applications, including effective water purification.

The electrospinning process is based on ejecting the polymer solution, which is the elemental makeup of the membrane, through an electric field and collecting it on an aluminum drum, as illustrated in Figure 11.

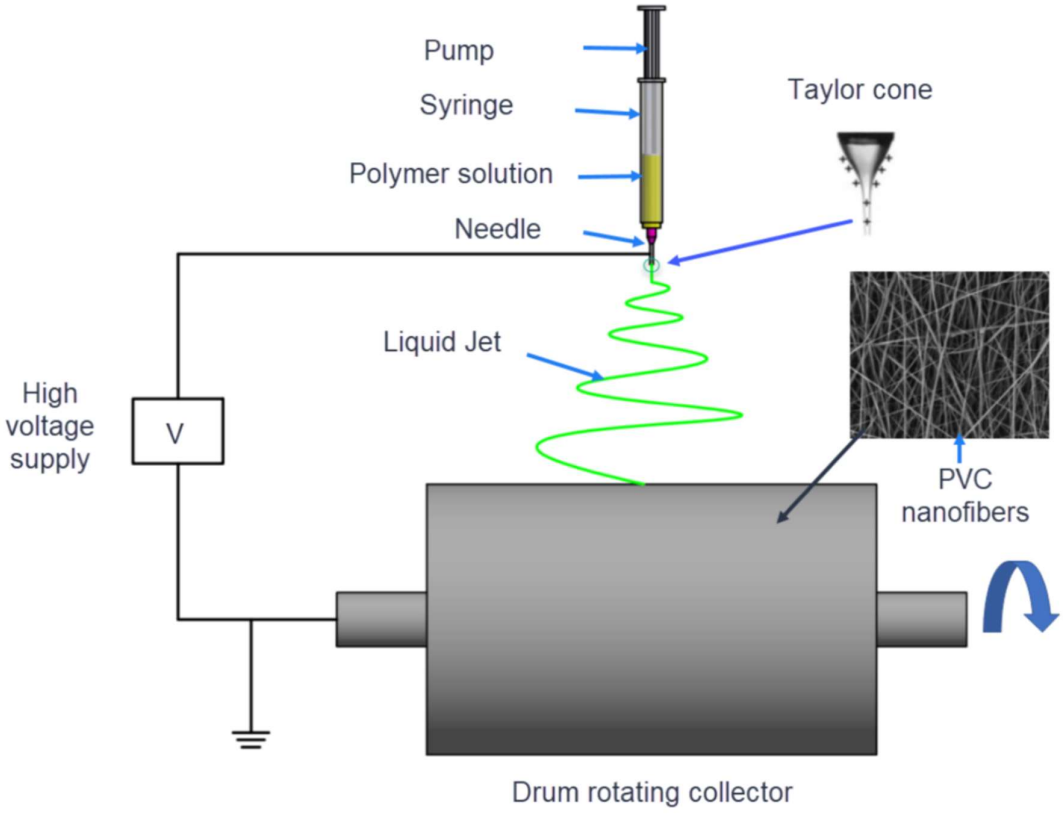

Figure 11. Electrospinning process (Pham et al., 2021)

The polymeric solution, namely its viscosity, volatility, and conductivity, first guides the morphology of the fibers to be fabricated. Furthermore, the morphology is influenced by several factors, which may be connected to the ambient humidity and temperature, as well as operational criteria such as the voltage utilized, the flow rate used, and the top-to-collector distance (Deitzel et al., 2001).

The electrospinning machine was used to produce a PVC membrane utilizing a solution composition specified in the results section. This PVC membrane was then modified; serving as the solid support for the organic ligand during water filtration.

D. Membrane Characterization

1. Scanning Electron Microscopy (SEM)

The surface parameters of the PVC membrane before and after modification were studied using a TESCAN VEGA 3 LMU scanning electron microscope (SEM). The sputtering coater was first employed to coat samples with a 10 nm platinum layer over a 10-minute period. Coated samples were subsequently examined using a scanning electron microscope (SEM) with a beam voltage of 5 kV and a working directory of 15 mm, and various magnification levels were observed, including 50 µm, 20 µm, 10 µm, and 5 µm. SEM images provide visual confirmation of the membrane modification according to visible fiber characteristics such as size, porosity, and distribution.

2. Energy Dispersive X-ray (EDX)

Energy dispersive X-ray (EDX) was used as a qualitative method to detect the elemental composition of the membrane and offer a reflective analysis of the elemental composition of the samples, using the same samples that have been submitted to SEM analysis. To have excitation energy that could cover a wide spectrum of elements, EDX was performed using a beam voltage of 30 kV. The EDX procedure was carried out on a specific point or portion of the membrane chosen to be representative of the entire membrane composition. The various elements identified in the sample are represented by an EDX-generated spectrum of peaks.

3. Water Contact Angle

The contact angle (CA) of water droplets on PVC membranes before and after modification was tested to determine the membranes' hydrophilicity. PVC membranes are hydrophobic, with a contact angle of around 135° (Asmatulu et al., 2013), which is one of their key limitations in water treatment methods (Wu et al., 2018). The modification process changes the membrane surface morphology, potentially enhancing the hydrophilicity of the membrane based on the utilized ligand.

A goniometer (OCA 15EC, DataPhysics, Germany) was utilized to measure the CA at room temperature. Membrane samples were put on a flat glass surface, and 5 µm water droplets were dripped over the membrane surface. The CA is then computed by the SCA 20 software, and a hydrophilic surface is indicated if CA falls less than 90° (Parvate et al., 2020). CA was measured ten times at different places for each sample and then averaged.

4. Pore Size Distribution

A capillary flow porometer (CFP-1100, Porous Material Inc. (PMI), USA) was used to measure the membrane pore size distribution for the PVC membranes before and after modification. The thickness of the membrane was initially measured and input into the testing program. The membrane sample was then placed in the specimen chamber and soaked in Galwik wetting liquid before being sealed. Subsequently, air was passed through with decreasing differential pressure. The fluid displaces out of the pore when the pressure is high enough to overcome the capillary forces of the fluid. As a result, the pressure was increased until all pores lose their fluid and become dry. The pore size distribution was then computed using the measured flow rate and gas pressure.

5. Thermogravimetric Analysis (TGA)

The thermal stabilities of the electrospun membrane pre and post-modification were determined using a thermogravimetric analyzer (TGA) and a Netzsch TG 209 F1 Libra instrument. Samples were heated from 30-800 °C under dynamic nitrogen flow at a heating rate of $10\ \mathrm{K.\,min^{-1}}$.

E. Atomic Absorption Spectroscopy

Atomic absorption spectroscopy (AAS) is a technique used in analytical chemistry to estimate the concentration of an element in aqueous solutions, particularly metals. Based on light absorption at a particular wavelength peculiar to the element, AAS determines the concentration of a present heavy metal in solution. An ICE 3000 series AAS was used to first develop a linear regression equation to determine the concentration from light absorption, using standards of known concentrations and their subsequent absorptions, which was then used to determine the concentration in water samples treated with the modified PVC membranes. The schematic diagram of the instrument's components is depicted in Figure 12.

The concentrations of lead(II), mercury(II), silver(II), and cadmium(II) ions in solution were determined using an air acetylene flame. The AAS detection limits for these metals are outlined in Table 3.

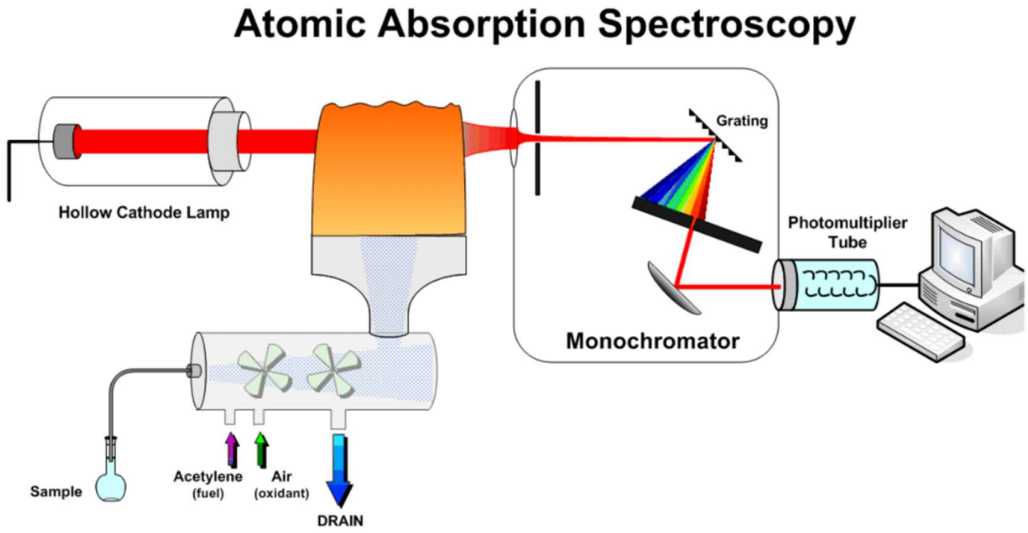

Figure 12. Schematic illustration of the AAS components

The AAS would yield an absorbance of 0 for a metal concentration of 0 ppm, an absorbance of 1 for the limit concentration, and any linear interpolation in between. To achieve optimal accuracy, treated water samples (of lead, silver, and cadmium) were diluted and compared to the 75th percentile of their respective detection ranges, whereas mercury water was analyzed without dilution.

Table 3. AAS detection limits

Metal	**AAS Detection Limit (ppm)**
Lead	17.5
Mercury	750
Silver	6.25
Cadmium	3.75

CHAPTER IV

RESULTS AND DISCUSSION: TCH-PVC MEMBRANE

The complexation of the organic ligand thiocarbohydrazide (TCH) with heavy metals was first investigated. The stoichiometry and binding constants were determined after detecting complex formation with UV-Vis spectroscopy. Following the formation of a heavy metal (HM)-TCH association, TCH was suspended on the surface of an electrospun PVC membrane and assessed for heavy metals removal from solution.

This chapter analyzes and reports on the effect of the alteration on the physicochemical properties of the membrane, including physical characteristics, elemental composition, hydrophilicity, and porosity. This study then investigates the potential of the TCH-PVC membrane for heavy metals removal from water.

A. Formation of Heavy Metal-TCH Complexes

1. Detection of Heavy Metal-TCH Complexes using UV-Vis Spectroscopy

Considering that metal removal is directed by chemical complexation with the ligand, the formation of the heavy metal-TCH complexes was investigated using a UV-Vis spectrophotometer. Considering TCH-based ligands are known to form complexes with iron(II) (Abu-Hussen and Emara, 2004), a UV-Vis investigation of Fe(II)-TCH complexation was utilized as a benchmark for the development of heavy metal-TCH complexes.

a. Fe(II)-TCH Complex

As iron(II) does not show an absorption pattern at the UV-Vis spectrum, a solution of the TCH ligand was titrated with iron(II) triflate in methanol to explore the

complexation of the metal to the ligand to form the metal-organic complex (Fe(II)-TCH). The titration was carried out by adding increasing concentrations of iron(II) triflate (0.5-10 equivalence) to a 9.421×10^{-5} M TCH methanol solution. Titration was performed sequentially using aliquots corresponding to different molar equivalents to TCH in solution, and UV measurements were acquired at each titration step, as indicated in Figure 13. Throughout the titration process, all samples were treated to identical physical (room temperature) and chemical conditions.

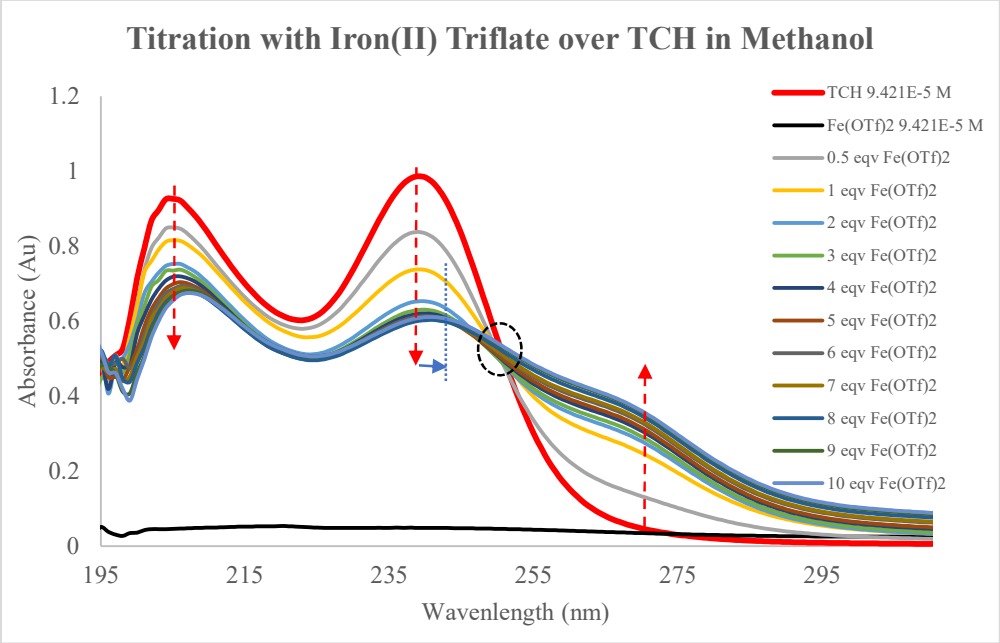

Figure 13. UV-visible absorbance spectra of TCH (9.421×10^{-5} M) titration with iron(II) triflate in methanol at room temperature

The two broad peaks of the TCH ligand (red spectrum), at 205 nm and 240 nm, decreased with each titration increment, with a new enhancing peak appearing at 270 nm. Furthermore, the broad peak of the TCH at 240 nm shifted during the titration. The peak's bathochromic shift, together with the hypochromic shifts of the two broad peaks and the amplification of the absorbance at 270 nm, resulted in the creation of a well-

defined isosbestic point at 251 nm. The discrepancy between the absorption spectrum of the Fe(II)-TCH mixture and the uncomplexed ligand spectrum, in addition to the emergence of the isosbestic point, suggests the complexation of the ligand with Fe(II) ions in the methanol solution. For relevance to the research field of water treatment, the titration was conducted in a mixed solvent solution of 1:1 methanol:water (Figure 14), and a 100% water solution (Figure 15).

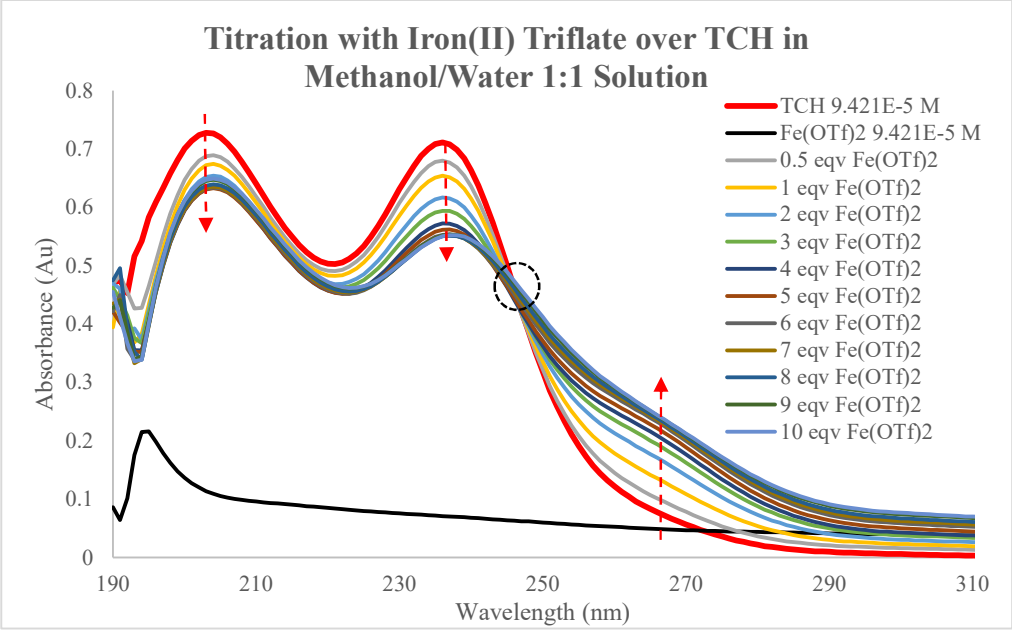

Figure 14. UV-visible absorbance spectra of TCH (9.421×10^{-5} M) titration with iron(II) triflate in methanol/water 1:1 solution at room temperature

The titration in the 1:1 methanol:water solution had similar results to the 100% methanol solution. This is important for applying the research findings to the treatment of industrial wastewater effluents, which may be contaminated with methanol (Gao et al., 2021) and often include increased amounts of iron and other heavy metals (Ajiboye et al., 2021).

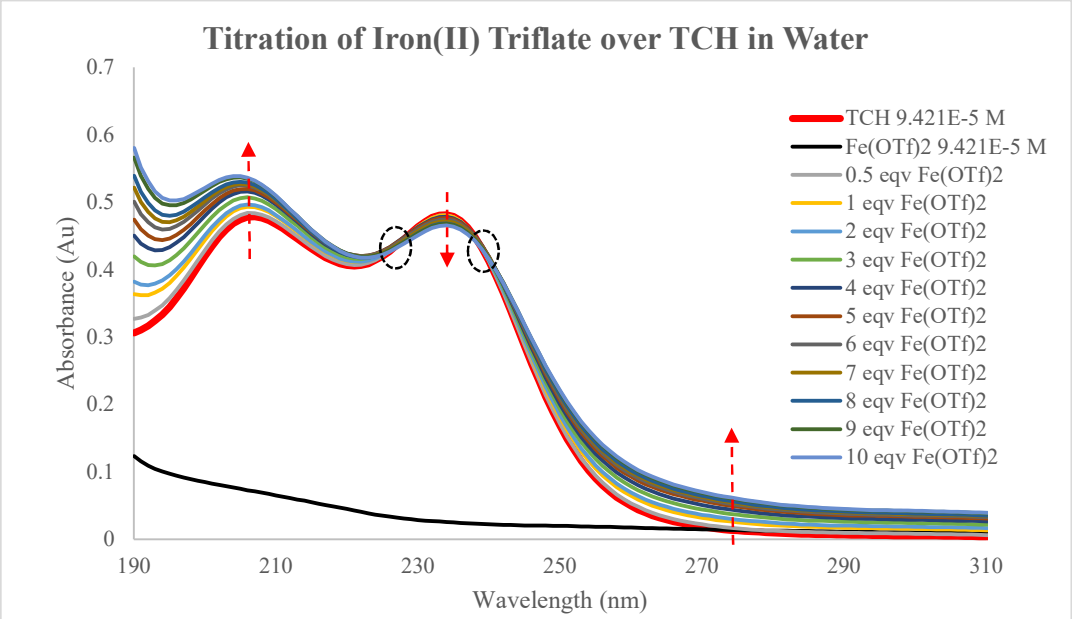

Figure 15. UV-visible absorbance spectra of TCH (9.421×10^{-5} M) titration with iron(II) triflate in water at room temperature

The same titration was conducted in a water solution, however, this yielded different findings from the titration in methanol. The TCH peak at 205 nm underwent a hyperchromic shift, as opposed to the hypochromic shift observed in the methanol solution titration. Consistent with the methanol titration, the wide peak at 240 nm showed a hypochromic shift as well as absorbance enhancement beyond the 245 nm wavelength. The latter yielded two isosbestic points at 228 nm and 240 nm, rather than a single isosbestic point in methanol, indicating that the TCH ligand complexed with iron(II) ions in water. This is required in order to extensively utilize the findings of this study in water filtration, which is not confined to industrial effluents.

These titration studies were performed three times to ensure data correctness and repeatability, and identical titration findings were achieved.

b. Cd(II)-TCH Complex

Similar to the Fe(II)-TCH complex study, a TCH ligand solution was titrated with cadmium(II) nitrate to investigate Cd(II) complexation to the organic ligand (Cd(II)-TCH). Increasing quantities of cadmium(II) nitrate (0.1-2.0 equivalence) were added to a 9.421×10^{-5} M TCH water solution. Titration was carried out progressively using aliquots corresponding to different molar equivalents of TCH in solution, and UV measurements were taken at each titration phase, as shown in Figure 16. The TCH broad peak at 206 nm increased with each titration step, exhibiting a hyperchromic shift. The peak at 234, on the other hand, underwent a hypochromic shift, resulting in the formation of a well-defined isosbestic point. The difference in the absorption spectra of the Cd(II)-TCH mixture and the uncomplexed ligand spectrum, as well as the appearance of the isosbestic point, indicates that the ligand has complexed with Cd(II) ions in the water solution.

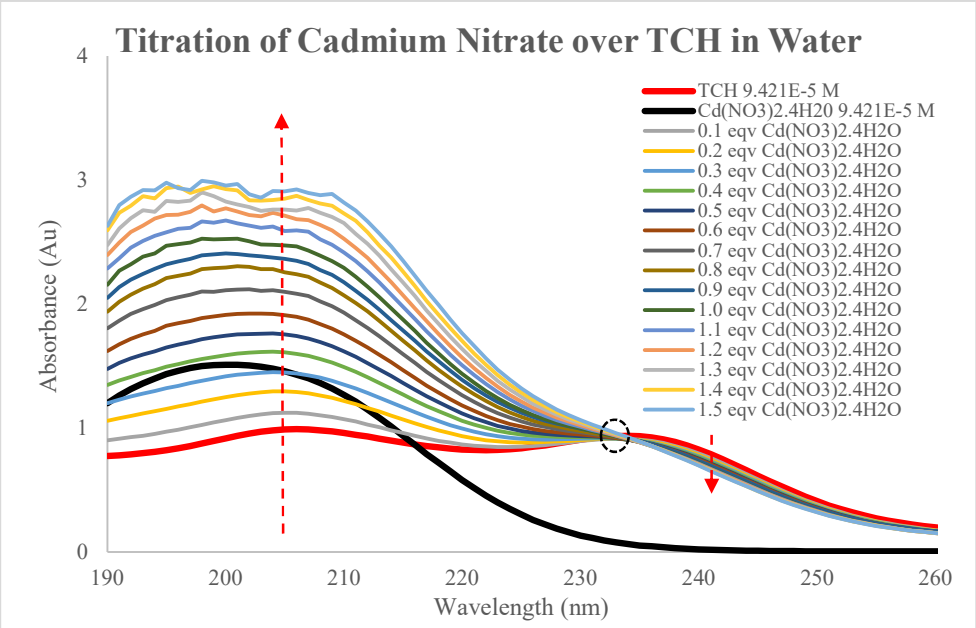

Figure 16. UV-visible absorbance spectra of TCH (9.421×10^{-5} M) titration with cadmium(II) nitrate in water at room temperature

c. Ag(I)-TCH Complex

To investigate the complexation of Ag(I) to the organic ligand (Ag(I)-TCH), the TCH ligand was titrated with silver(I) nitrate. The complexation was seen in the inverse titration; adding aliquots of the ligand to an Ag(I) solution for this experiment. Titration was performed by adding increasing amounts of TCH (0.1-2.0 equivalence) to a 9.421×10^{-5} M of silver(I) nitrate water solution (Figure 17). The absorbance at the two broad peaks underwent a hyperchromic shift, as well as hypsochromic on the 210 nm wavelength. Furthermore, the absorbance past 260 nm decreased in intensity, resulting in an isosbestic point at 263 nm. The difference in the absorbance spectrum and the isosbestic point show that the Ag(I)-TCH complex forms in water.

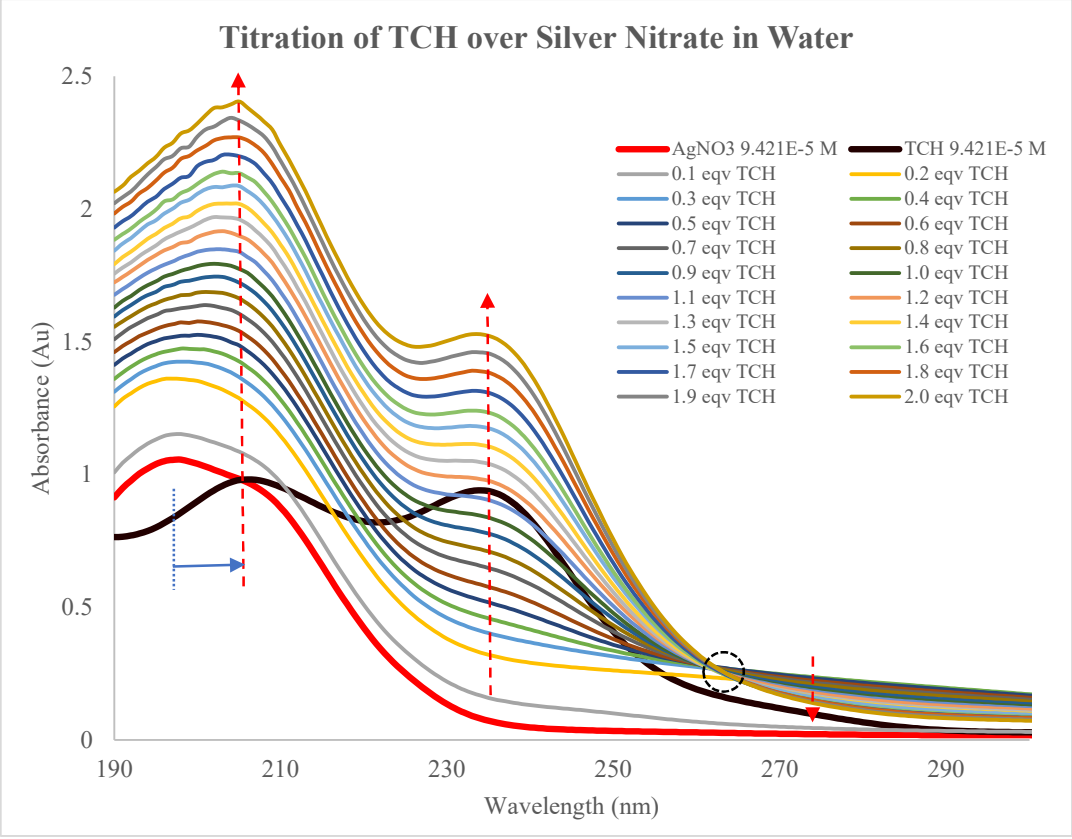

Figure 17. UV-visible absorbance spectra of silver(I) nitrate (9.421×10^{-5} M) titration with TCH in water at room temperature

d. Hg(II)-TCH Complex

To study the complexation of Hg(II) to the organic ligand TCH, a titration with increasing quantities of mercury ions in TCH solution (9.421×10^{-5} M) was performed (Figure 18). During the progress of the titration, the peak at 236 nm exhibited a hyperchromic shift. As observed, the enhancement in absorbance at this peak cannot be attributed to mercury, which does not have a peak absorbance at this wavelength. Furthermore, a new peak at 215 nm was observed to form. The difference between the new titrated absorption behavior and the uncomplexed TCH suggests that a Hg(II)-TCH complex forms in water.

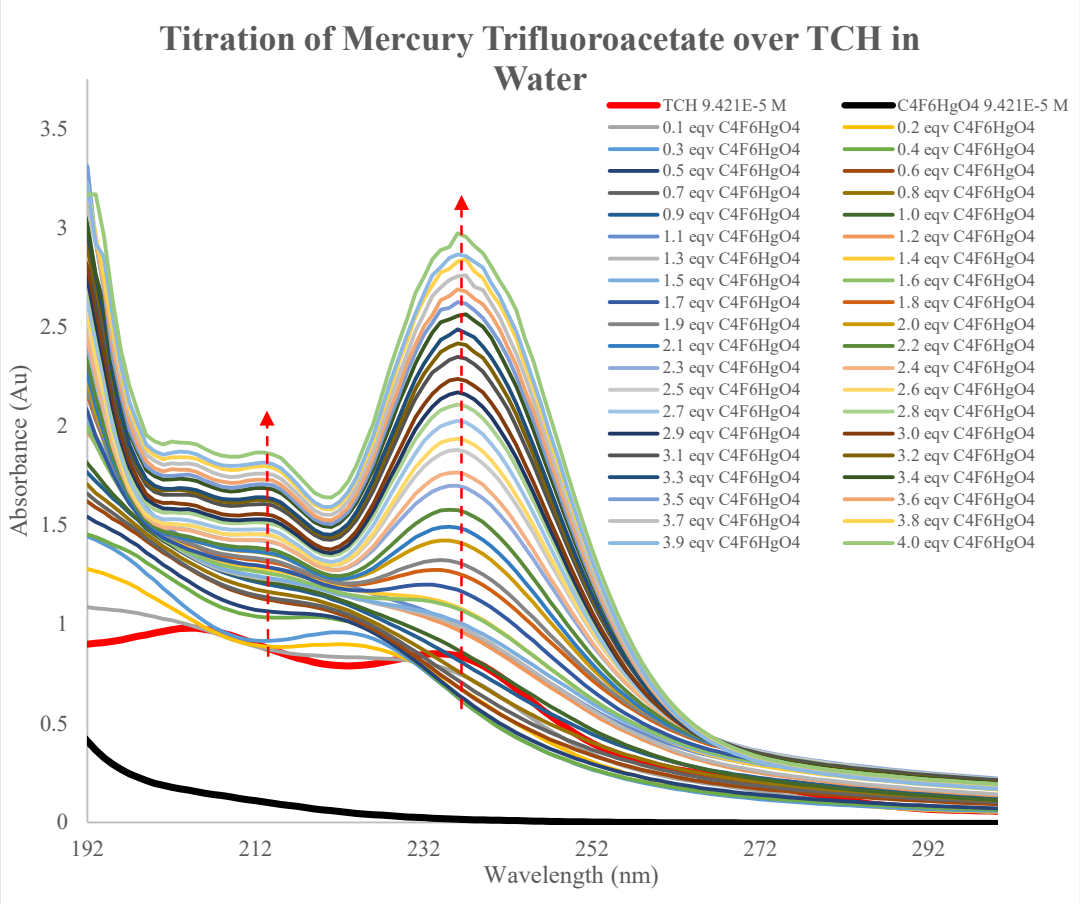

Figure 18. UV-visible absorbance spectra of TCH (9.421×10^{-5} M) titration with mercury(II) trifluoroacetate in water at room temperature

e. Pb(II)-TCH Complex

To investigate the complexation of Pb(II) to the organic ligand TCH, titration was performed by adding increasing amounts of lead (0.1-2.0 equivalence) to the TCH solution (9.421×10^{-5} M) (Figure 19), and the inverse titration; adding TCH (0.1-2.0 equivalence) to lead solution (9.421×10^{-5} M) (Figure 20). The peaks in both absorption spectra increased additively, with no alteration in absorbance behavior. The absence of an isosbestic point in both titration trials exacerbates the latter. This suggests that the TCH ligand does not establish coordination bonds with lead metal ions in solution and that the TCH-PVC membrane will not likely sequester Pb(II) from water.

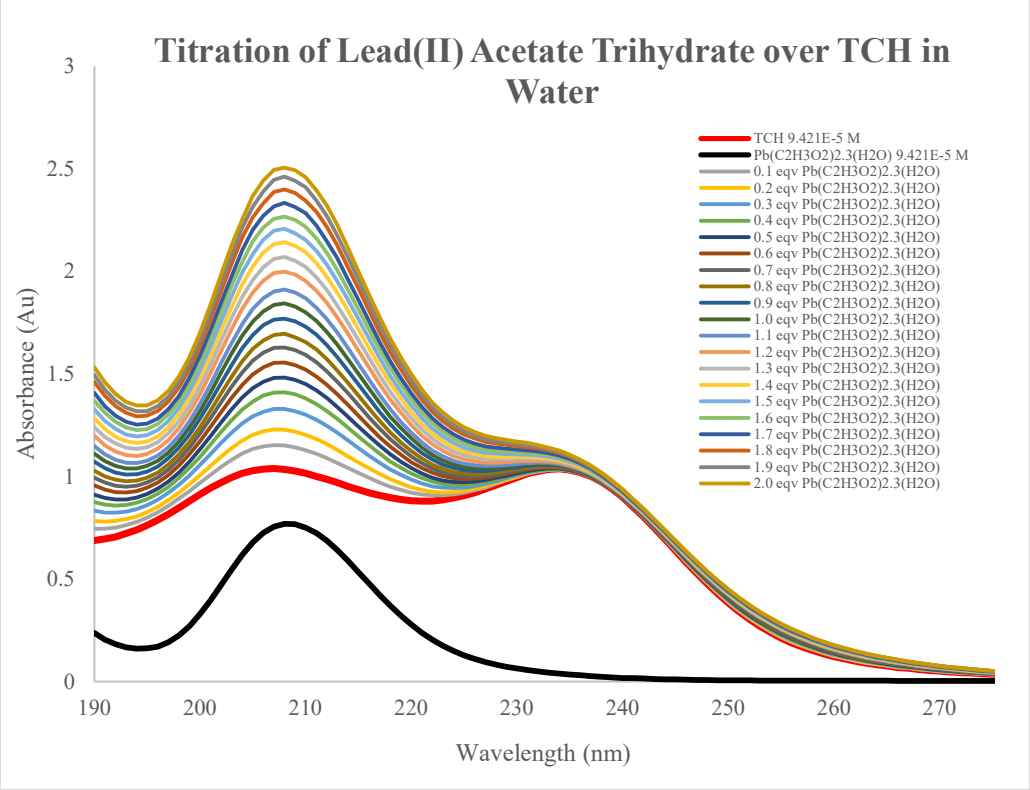

Figure 19. UV-visible absorbance spectra of TCH (9.421×10^{-5} M) titration with lead(II) acetate in water at room temperature

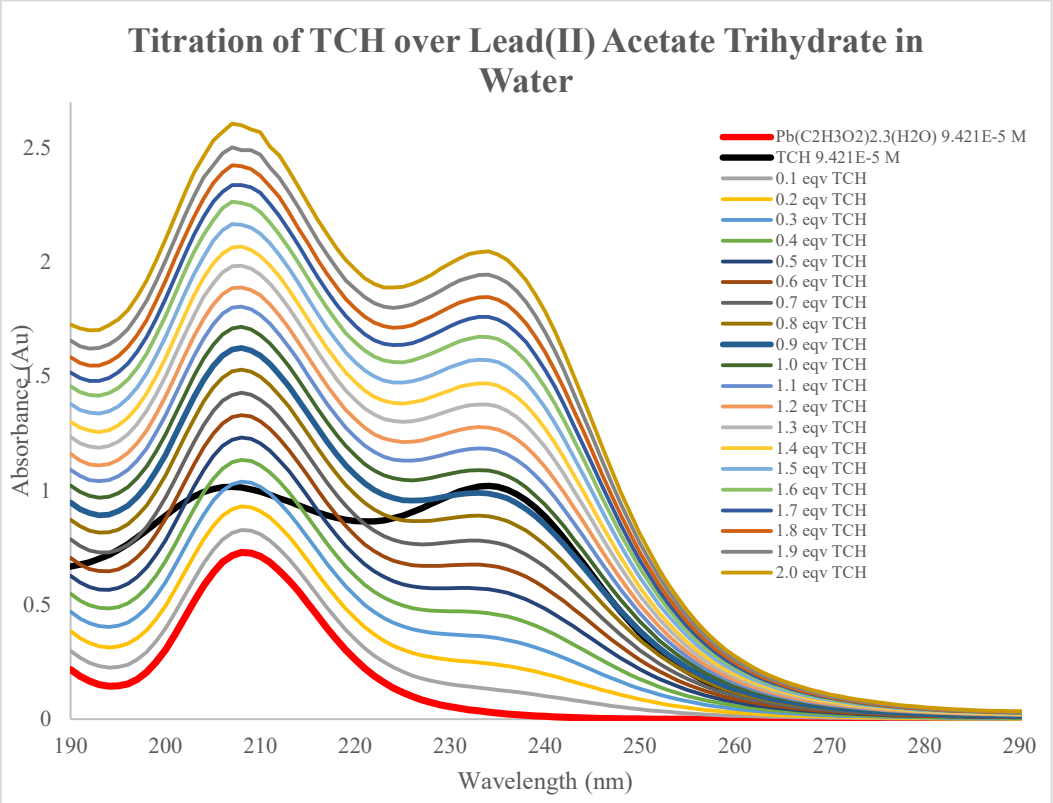

Figure 20. UV-visible absorbance spectra of lead(II) acetate (9.421×10^{-5} M) titration with TCH in water at room temperature

2. *Determination of Stability Constant*

Having confirmed the formation of TCH complexes with Fe(II), Cd(II), Ag(I), and Hg(II), the titration UV-Vis data was modeled to simulate the binding stoichiometry and affinity of the complexes, and to compute the stability constant for each complex accordingly. The absorption data were modeled using the Benesi-Hildebrand relationship for 1:1 complexes (eqn. (1)) and 1:2 complexes (eqn. (2)) (Benesi & Hildebrand, 1949):

$$\frac{1}{A - A_0} = \frac{1}{A_f - A_0} + \frac{1}{K_a[M](A_f - A_0)} \quad (1)$$

$$\frac{1}{A - A_0} = \frac{1}{A_f - A_0} + \frac{1}{K_a[M]^2(A_f - A_0)} \quad (2)$$

Where:

- $A_0, A, and\ A_f$: UV-Vis absorption values (Au) in the absence of, at the intermediate and, at the saturation of the interaction with the metal ions
- [M]: concentration of aqueous metal ion added [M]
- k_a: binding constant [M^{-1}]

For additional accuracy in the computations, eqn. (1) was further expanded to obtain a logarithmic transformation (eqn. (3)):

$$\frac{1}{A - A_0} = \frac{1}{A_f - A_0} + \frac{1}{K_a[M](A_f - A_0)}$$

$$\frac{A_f - A_0}{A - A_0} = 1 + \frac{1}{K_a[M]}$$

$$\log\left(\frac{A_f - A_0}{A - A_0}\right) = -(\log(K_a) + \log([M]))$$

$$\log\left(\frac{A_f - A_0}{A - A_0}\right) = \log([M]) + \log(K_a) \quad (3)$$

The UV-Vis data at the excitation wavelength was simulated using each of the three models, and the ones with the best linear correlation were deemed indicative of the metal-ligand complex binding stoichiometry. The logarithmic transformation (eqn. (3)) presented the highest linear correlation factor for all four complexes and was utilized to represent the binding at each complex's excitation wavelength, as illustrated in Figure 21. As a result, the four complexes maintain the 1:1 (metal:ligand) stoichiometry, and the appropriate binding constant (K_a) is calculated using eqn. (3) (Table 4).

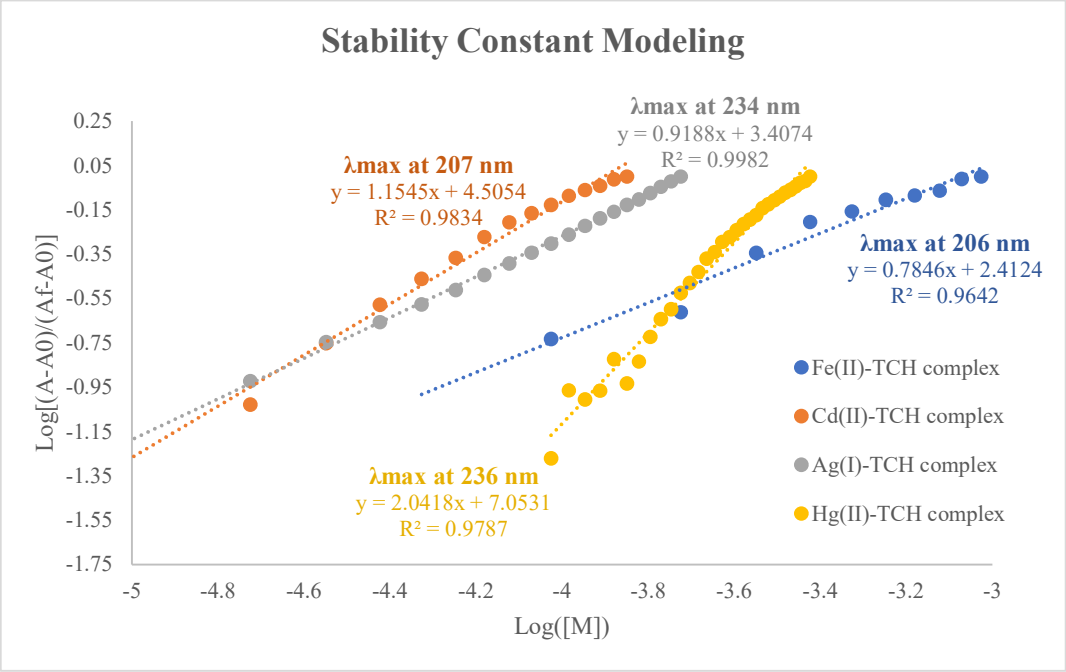

Figure 21. Benesi-Hildebrand plots for determination of binding constant of TCH for Fe(II), Cd(II), Ag(I), and Hg(II) ions

Table 4. Stability constant for metal-TCH complexes

Complex	$K_a\ [M^{-1}]$
Fe(II)-TCH	2.6×10^2
Cd(II)-TCH	3.2×10^4
Ag(I)-TCH	2.6×10^3
Hg(II)-TCH	1.13×10^7

According to their binding constant values, we may order the complex formation in order of decreasing binding strength as follows: Hg(II)-TCH > Cd(II)-TCH > Ag(I)-TCH > Fe(II)-TCH.

B. Preparation of Electro-spun PVC Membranes

Having detected heavy metals-TSC complexation in solution, a PVC electro-spun membrane was prepared to be used as solid support for the TCH ligand to sequester heavy metal ions from water.

An optimized solvent ratio of 62.5:37.5 DMF:THF and a PVC concentration of 16% by weight were used in the formulation of the PVC matrix to be used in the electro-spun membrane synthesis (Badran, 2019). The solvent was produced by mixing 7 mL of DMF with 4 mL of THF and adding 1.936 g of PVC to the mixture. The polymer solution was mixed overnight at room temperature using magnetic stirring at 600 rpm.

The aforementioned polymer solution was utilized to produce the membrane using a laboratory-scale electrospinning machine. The viscous polymer was injected into a 10 ml syringe and put on the equipment's metal capillary nozzle. To guarantee optimum synthesis with the pump rate (1 ml/hr), a thin tube and tip were employed. The electrospun fibers were pumped at a distance of 15 cm from the collector in an electric field of 18 kV. The fibers were collected on a cylindrical anodized aluminum drum with a diameter of 100 cm and a length of 200 cm that was programmed to revolve at 600 rpm. The membrane was prepared at room temperature and was designed to last 8 hours at the pump rate employed. The PVC membrane was physically characterized to ensure that appropriate electrospinning conditions were employed, and it was compared to the modified membrane characterization described later in this chapter.

C. PVC Membrane Functionalization

PVC membrane was modified by incorporating TCH ligands on its surface. The modification was accomplished by immersing the electrospun PVC membrane in a mixture of ethanol, deionized water, and dissolved TCH following the ratios outlined in Table 5.

Table 5. TCH-PVC membrane functionalization ratios

PVC (mg)	Ethanol (µl)	Water (µl)	TCH(mg)
1	150	50	5

The PVC:TCH and PVC:TSC ratios in Chapter V were optimized utilizing metal removal tests and using ratios ranging from 1:1-1:5. The removal testing revealed that a 1:5 ratio of TCH-PVC had the highest sorption effectiveness. The findings of this experiment, however, were influenced by a constant error caused by a contaminated batch of 0.45 m nylon filters used for subsequent ion concentration measurement by AAS, and hence the optimization results are not reported herein. The contamination was detected at an advanced stage in the research and eliminated from all subsequent testing, however, the optimization pattern was preserved. Notably, the high modification ratio was most likely necessary due to the TCH ligand's weak solubility and the terminal NH_2 group's poor nucleophilicity, which necessitates replacing a chlorine atom in the PVC fibers to achieve modification.

The mixture with the PVC membrane was placed in an oil bath and heated overnight at 65°C. Following this, the modified membrane was washed with ethanol and distilled water before being allowed to dry at room temperature.

The degree of modification was determined by comparing the weight of the membrane from unmodified PVC to modified TCH-PVC. Furthermore, the

modification solvent was dried, and the amount of residual ligand was determined. The difference in ligand amount was estimated and compared to the change in membrane mass, which was found to be of comparable magnitudes. The average degree of modification was found to be around 1:1.3 $\pm$ 0.2 (Table 6).

Table 6. Degree of PVC modification by the TCH ligand

PVC (mg)	TCH-PVC (mg)	Increase in Mass (mg)	Ligand Consumed (mg)	Degree of Modification
24.5	52.3	27.8	31.8	1:1.3 $\pm$ 0.2

D. Characterization of TCH-PVC Membranes

Physicochemical characterization tests on the TCH-PVC membrane were performed and contrasted against control PVC samples to validate the functionalization process.

1. Physical and Elemental Characterization: SEM and EDX Analysis

TCH-PVC and non-functionalized PVC membranes were analyzed by SEM to assess the influence of the functionalization on the fibers' morphology. Furthermore, EDX was utilized to confirm the elemental composition of membrane samples, namely the presence of sulfur and nitrogen; confirming the modification process. For both tests, samples were coated with a 10 nm layer of platinum.

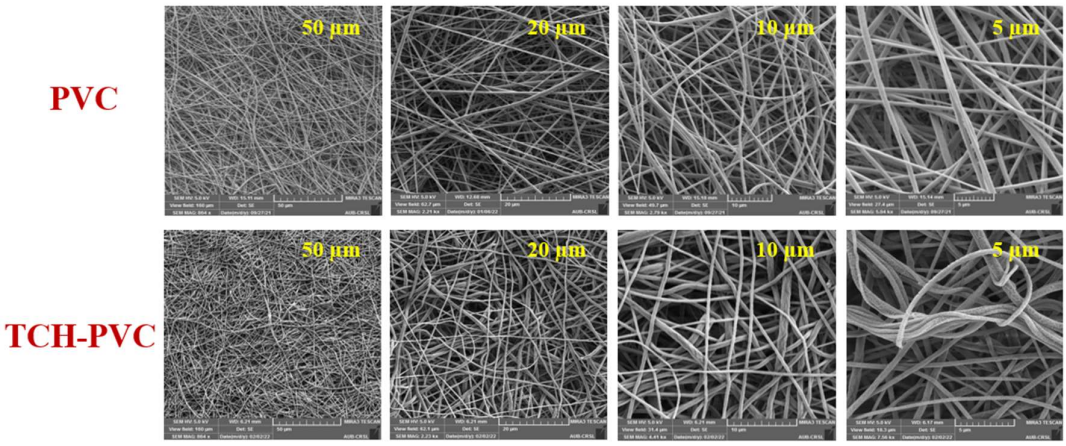

Figure 22. SEM images of PVC and TCH-PVC nanofibers

The PVC nanofibers exhibit constant thickness and are consistently dispersed, with no bulging, as revealed in the SEM images (Figure 22), indicating that suitable preparation mixture and conditions were followed.

The SEM images of TCH-PVC demonstrate that the modification had an effect on membrane morphology, with the spacing between fibers reduced and their entanglement increased. The latter can be due to hydrogen bonding, which validates the functionalization process. Furthermore, the presence of sulfur was observed in the EDX spectra (Figure 23), validating the prior.

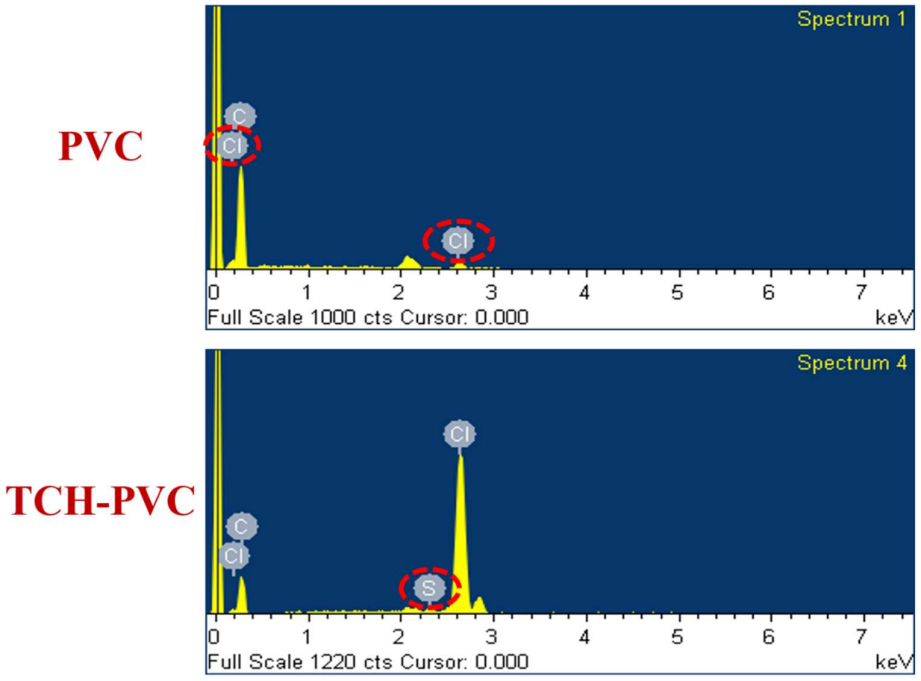

Figure 23. EDX spectra of PVC and TCH-PVC nanofibers

2. Pore Size Distribution and Water Contact Angle

The pore size distribution of the PVC membrane before and after modification was measured, as shown in Figure 48 in Appendix I. The average pore size diameter of the PVC membrane was determined to be 2.86 µm, which was more than that of the TCH-PVC, which was 2.79 µm. The reduction in pore size distribution corresponds to the rise in fiber entanglement seen in the SEM investigation. Furthermore, this decrease in porosity may result in increased adsorption capacity (Jamshidi Gohari et al., 2015). This is due to the increase in the adsorbent's surface area that would react with the adsorbate.

Notably, Asmatulu et al. (2018) demonstrated that the larger the electrospun membrane thickness, the smaller the pore size. This was consistent with our findings, where the thickness of the functionalized TCH-PVC membrane was larger than that of

the PVC membrane (Table 7). Subsequently, the former had a lower average pore size than the latter.

Table 7. Thickness and pore size distribution

Parameter	**PVC**	**TCH-PVC**
Mean Pore Diameter (µm)	2.86	2.79
Average Thickness (µm)	105 ± 11	196 ± 13

In order to investigate the effect of membrane functionalization on the hydrophilicity of the membrane, the water contact angle was measured for PVC and TCH-PVC membranes (Figure 24). The functionalization of the PVC membrane had a negligible effect on the membrane hydrophilicity, as shown in Table 8. Although the introduction of polar amine groups (N-functional groups), which are present in the TCH ligand, is expected to reduce membrane hydrophobicity (Dai et al., 2009), this was not the case in this modification due to the relatively small chains, which correlated with the small average membrane pore size, which itself decreased with the modification. Furthermore, the smaller the pore size, the greater the membrane wettability resistance (McGaughey, 2020). As a result of this, the incorporation of the TCH ligand onto the PVC membrane surface in conjunction with a reduction in pore size diameter resulted in the latter's nullification of the former's hydrophilic enhancement of the fibers.

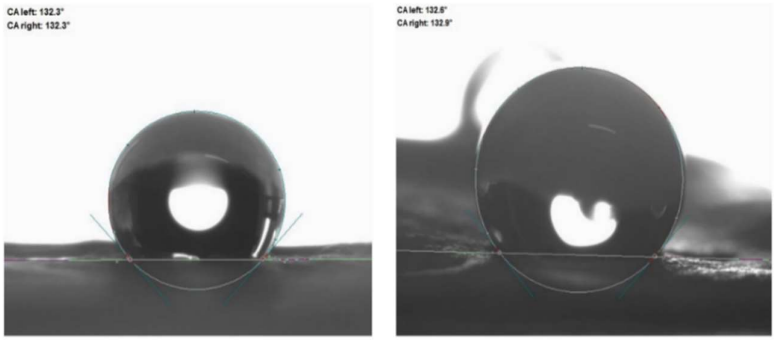

Figure 24. CA measurements for PVC and TCH-PVC membranes

Table 8. PVC and TCH-PVC CA results

Parameter	**PVC**	**TCH-PVC**
Range	128.0°-138.0°	118.4°-144.0°
Mean	132.6°	132.5°

E. Removal Efficiency of Heavy Metal Ions from Water

Having confirmed the formation of metal-TCH complexes in solution and characterizing their binding stoichiometry and affinity, and successful modifying the surface of PVC membranes with the TCH ligand, we proceeded with testing the adsorption capabilities of the modified membranes towards silver(I), mercury(II), lead(II), and cadmium(II) ions. We predicted that the chemisorption efficiency might follow the order of binding strength based on the results of the stability constants. At the same time, we anticipated that this may not be the case since the binding motif found in the titration tests differs when the ligand is suspended on the fibers, as the latter involves the substitution of a functional group in the ligand (the terminal NH_2).

1. Silver(I) Removal

The removal efficacy of the functionalized membrane was evaluated using a 100 ppm solution of silver(I) in water. TCH-PVC membrane (20 mg) was immersed in 10 ml of silver(I) solution and shaken for 24 hours at room temperature and neutral pH at 600 rpm. Treated water samples were collected after 10 minutes, 20 minutes, 30 minutes, 1 hour, 2 hours, 5 hours, and 24 hours to determine removal ability using atomic absorption spectroscopy (AAS). For this experiment, a calibration curve was built using seven standard solutions with known silver(I) content with a coefficient of determination of 99.75%, as shown in Figure 50 in Appendix II.

As demonstrated in Figure 25, TCH-PVC membrane removed around 40% of silver(I) ions from the solution in just 10 minutes. Unmodified PVC membrane had negligible (< 1%) silver removal; confirming silver removal as a result of silver chemical chelation via the TCH ligand.

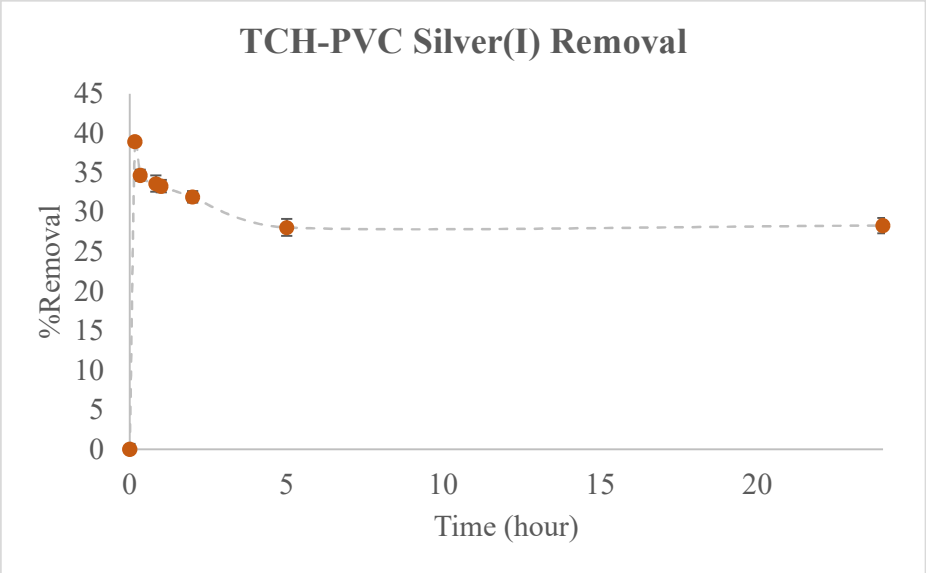

Figure 25. Percentage removal of Ag(I) from solution ([Ag]=100 ppm, at room temperature, and pH=7)

The treated membranes were then rinsed with distilled water and dried before being examined with SEM and EDX (Figure 26). The TCH-PVC membrane employed in treatment had a sensing effect compared to the unmodified PVC utilized in silver sorption (Figure 26-(a) & (b)). Additionally, SEM micrographs detected silver structures on the TCH-PVC fibers which were confirmed by EDX. Our findings are consistent with the identification of heavy metals on nanofibers reported in recent membrane filtration investigations (Youness, 2021), indicating chemical sorption of the metals on the membrane's surface.

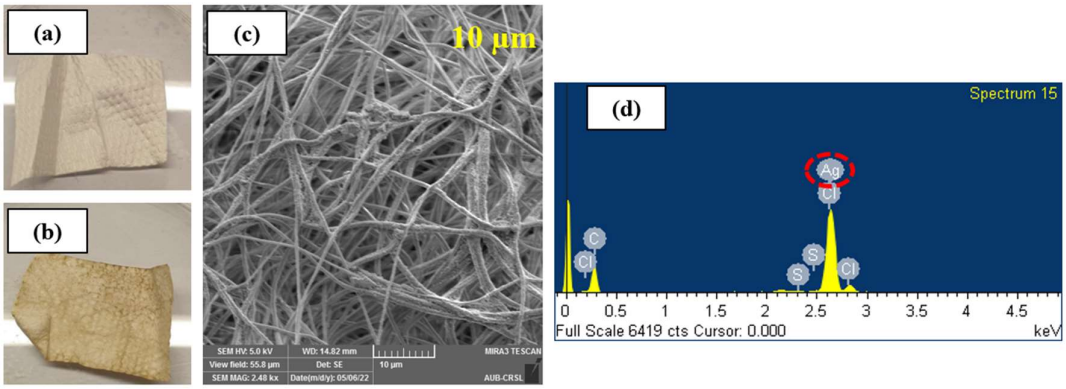

Figure 26. Physical analysis of membranes used in silver sorption (a) PVC-Ag, (b) TCH-PVC-Ag membrane sensing, (c) SEM micrograph of TCH-PVC-Ag, and (d) EDX spectra of TCH-PVC-Ag

2. *Mercury(II) Removal*

Similar to silver(I) removal testing, 20 mg of TSC-PVC membrane was immersed in 10 ml of a 100 ppm mercury(II) solution in water and shaken at 600 rpm for 24 hours. Figure 51 in Appendix II depicts the preparation of a calibration curve for

mercury concentration using six standard solutions (R^2= 99.97%). The TCH-PVC membrane absorbed 70.32% of the mercury(II) ions from the solution

Mercury removal was negligible (<3%) in unmodified PVC membranes, indicating mercury removal as a result of the incorporation of the TCH ligand into the membrane fibers, which then interacted with mercury in solution.

The membranes used to adsorb mercury ions were similarly examined with SEM and EDX (Figure 27). Compared to the unmodified PVC used in mercury removal, the TCH-PVC membrane used in treatment exhibited a sensing effect (Figure 27-(a) & (b)). Additionally, SEM micrographs detected mercury components on the TCH-PVC fibers which were confirmed by EDX.

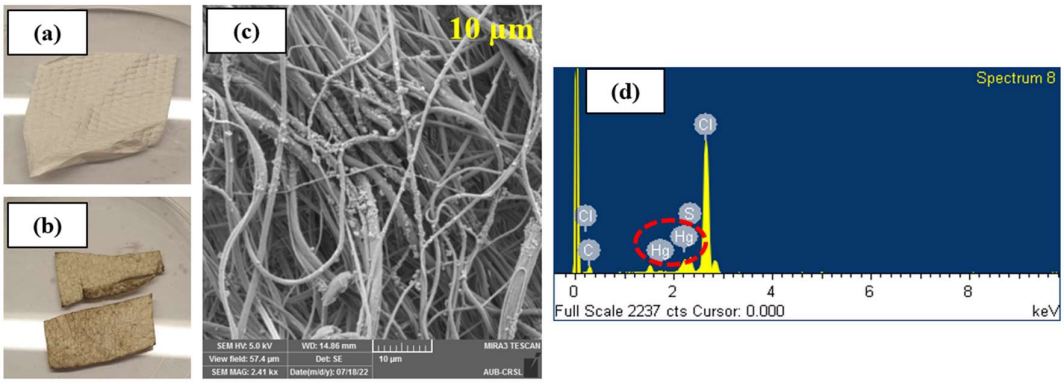

Figure 27. Physical analysis of membranes used in mercury sorption (a) PVC-Hg, (b) TCH-PVC-Hg membrane sensing, (c) SEM micrograph of TCH-PVC-Hg, and (d) EDX spectra of TCH-PVC-Hg

3. Lead(II) and Cadmium(II) Removal

TCH-PVC membrane (20 mg) was immersed in 10 ml of 100 ppm lead(II) and cadmium(II) monoionic water solutions in water and shaken at 600 rpm for 24 hours. Figures 52 and 53 in Appendix II depict the preparation of lead and cadmium concentration calibration curves. AAS analysis demonstrated no removal of lead(II) and

cadmium(II) ions from solution after 24 hours. This was anticipated for lead(II) since it was not found to form complexes with the TCH ligand, but not for cadmium(II) as it established coordination bonds with TCH. The removal of lead(II) and cadmium(II) utilizing TCH might be improved by incorporating aldehyde into the membrane functionalization, since metal chelation between the pyridine-sulfur coordination could occur.

Because TCH-PVC had relatively low removal effectiveness of Ag(I) and Hg(II), as well as a low equilibrium for Ag(I), the heavy metals sorption analysis was limited and subsequent experiments were directed to the TSC-PVC membrane, which demonstrated superior sorption efficiency, as shown in Chapter V.

CHAPTER V

RESULTS AND DISCUSSION: TSC-PVC MEMBRANE

Initially, the interaction of the organic ligand thiosemicarbazide (TSC) with heavy metals was investigated. The stoichiometry and binding constants were determined after detecting complex formation with UV-Vis spectroscopy. Following the formation of heavy metal-TSC associations, TSC was suspended on the surface of an electrospun PVC membrane to be assessed for heavy metal removal from solution.

This chapter analyzes and reports on the effect of the alteration on the physicochemical properties of the membrane, including physical characteristics, elemental composition, hydrophilicity, porosity, and thermal stability. This study then investigates the potential of the TSC-PVC membrane for heavy metals removal from water.

A. Formation of Heavy Metal-TSC Complexes

1. Detection of Heavy Metal-TSC Complexes using UV-Vis Spectroscopy

The formation of the heavy metal-TCH complexes was investigated using a UV-Vis spectrophotometer. The formation of such complexes would proceed metal chelation in the subsequent water filtration analysis.

a. Ag(I)-TSC Complex

To investigate the complexation of Ag(I) to the organic ligand (Ag(I)-TSC), a water solution of the TSC ligand was titrated with silver(I) nitrate. Titration was

performed by adding increasing amounts of silver(I) nitrate (0.1-1.5 equivalence) to a 1.097×10^{-4} M of TSC water solution (Figure 28).

The absorbance at the broad peak at 200 nm underwent a hyperchromic shift, as well as a hypochromic shift at 236 nm; resulting in the creation of an isosbestic point at 230 nm. Furthermore, the absorbance past 247 nm increased in intensity, resulting in a second isosbestic point at 247 nm. The difference in the absorbance spectrum and the formation of two isosbestic points show that the Ag(I)-TSC complex forms in water.

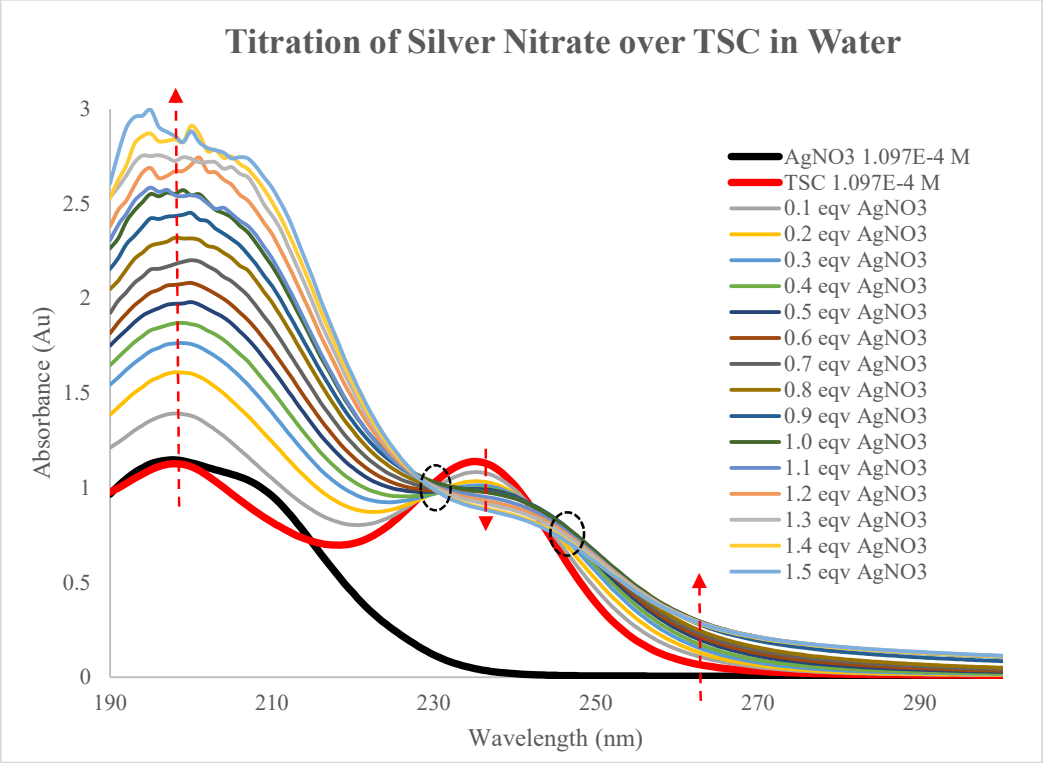

Figure 28. UV-visible absorbance spectra of TSC (1.097×10^{-4} M) titration with silver(I) nitrate in water at room temperature

b. Hg(II)-TSC Complex

To investigate the complexation of Hg(II) to the organic ligand (Hg(II)-TSC), a 1.097×10^{-4} M water solution of the ligand was titrated with the sequential addition of mercury(II) trifluoroacetate.

Up to the addition of 0.5 equivalence of mercury(II) trifluoroacetate, the absorbance spectrum displayed a well-defined behavior of hyperchromic shift prior to 230 nm and hypochromic shift post it, resulting in the formation of an isosbestic point at 230 nm (Figure 29).

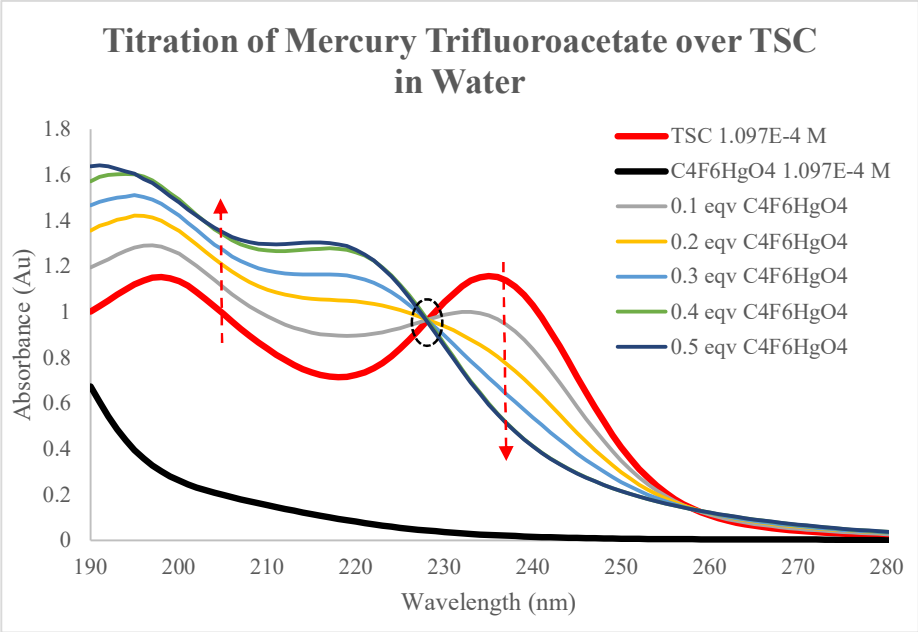

Figure 29. UV-visible absorbance spectra of TSC (1.097×10^{-4} M) titration with mercury(II) trifluoroacetate (0.5 eqv.) in water at room temperature

The absorbance behavior altered as more mercury(II) trifluoroacetate was added. The new absorbance spectrum alternates three times between hyperchromic, hypochromic, and hyperchromic shifts, yielding two new isosbestic spots at 200 and 205 nm (Figure 30).

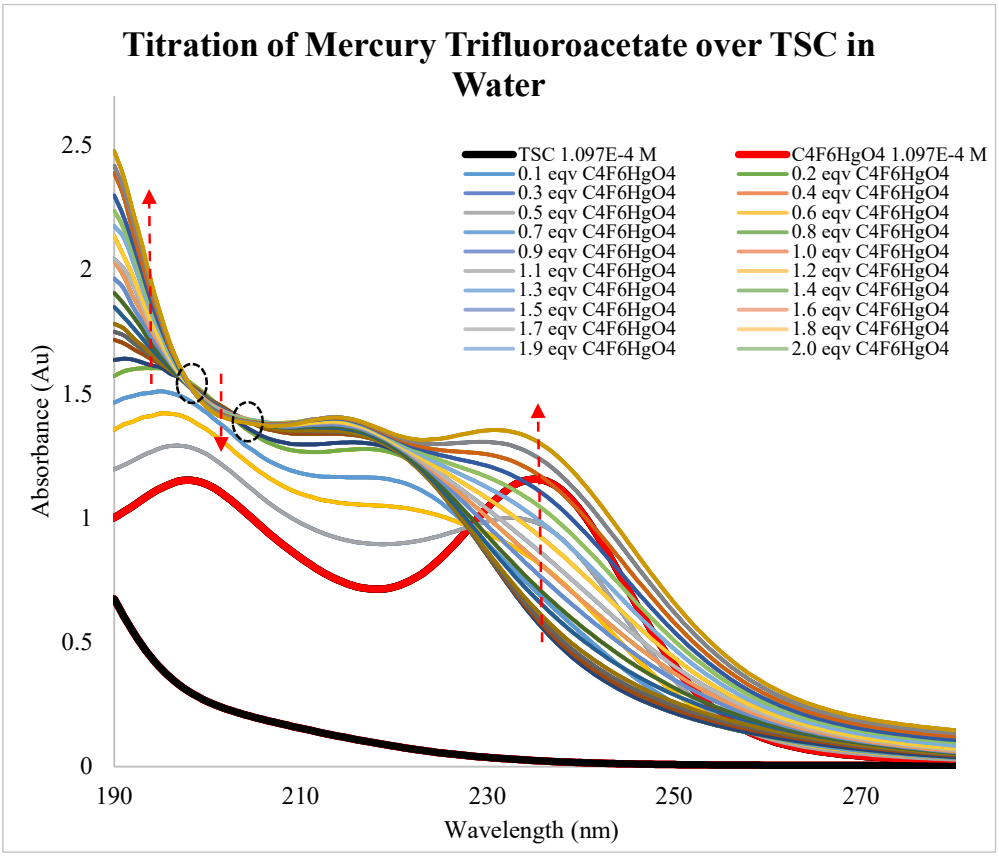

Figure 30. UV-visible absorbance spectra of TSC (1.097×10^{-4} M) titration with mercury(II) trifluoroacetate (2 eqv.) in water at room temperature

The variation in absorbance spectra might be caused by distinct binding motifs. Mercury has prismatic structures that are tetrahedral (four coordination bonds) and octahedral (six coordination bonds). For this, one binding motif may have predominated up to the addition of 0.5 eqv. of mercury, while another binding motif may have predominated after this point. This expands the possibilities of having multiple binding motifs or a hybrid of the latter.

2. *Determination of Stability Constant*

Having confirmed the formation of TSC complexes with Ag(I) and Hg(II), the titration UV-Vis data was modeled to simulate the binding stoichiometry and affinity of

the complexes, and to compute the stability constant for each complex accordingly. The absorption data were modeled using the Benesi-Hildebrand relationship (eqn. (1), (2), & (3)). The logarithmic transformation (eqn. (3)) presented the highest linear correlation factor for both complexes and was utilized to represent the binding at each complex's excitation wavelength, as illustrated in Figure 31. Accordingly, the two complexes maintain the 1:1 (metal:ligand) stoichiometry, and the appropriate binding constant (K_a) is calculated using eqn. (3) (Table 9).

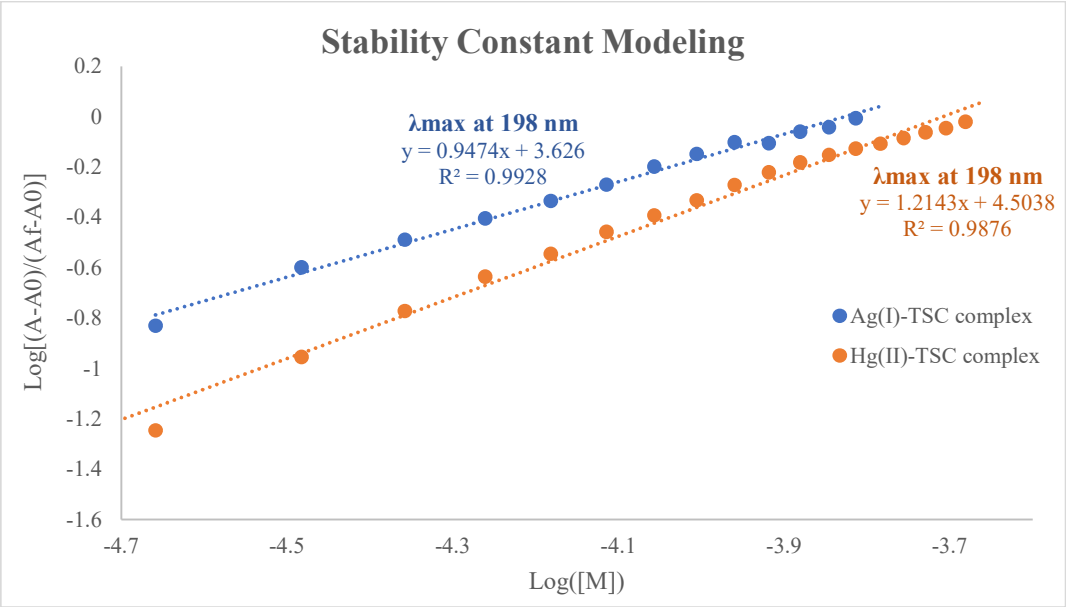

Figure 31. Benesi-Hildebrand plots for determination of binding constant of TSC for Ag(I) and Hg(II) ions

Table 9. Stability constant for metal-TSC complexes

Complex	$K_a\ [M^{-1}]$
Ag(I)-TSC	4.2×10^3
Hg(II)-TSC	3.2×10^4

According to their binding constant values, we may order the complex formation in order of decreasing binding strength as Hg(II)-TSC > Ag(I)-TSC.

B. Modification of PVC Membrane with TSC

PVC membrane was prepared to the same conditions in the previous chapter and functionalized to achieve the addition of the TSC ligand on its surface. Functionalization was accomplished by immersing the PVC membrane in a mixture of ethanol, deionized water, and dissolved TSC, utilizing the ratios in Table 10.

Table 10. TSC-PVC membrane modification ratios

PVC (mg)	Ethanol (µl)	Water (µl)	TSC (mg)
1	150	50	3

The mixture with the PVC membrane was placed in an oil bath and heated overnight at 65°C. Following this, the modified membrane was washed with ethanol and distilled water before being left to dry at room temperature. The modification yield was determined by comparing the weight of the membrane from unmodified PVC to modified TSC-PVC. Additionally, the modification solvent was dried, and the amount of residual ligand was determined. The difference in ligand amount was computed and compared to the change in membrane mass, which was found to be of comparable magnitudes. The average degree of modification of PVC with the TSC ligand was found to be around 1:0.5 $\pm$ 0.15 (Table 11).

Table 11. Degree of PVC modification by the TSC ligand

PVC (mg)	TSC-PVC (mg)	Increase in Mass (mg)	Ligand Consumed (mg)	Degree of Modification
44.6	63.3	18.4	20.8	1:0.5 $\pm$ 0.15

C. Characterization of TSC-PVC Membrane

Physicochemical characterization tests on the TSC-PVC membrane were performed and contrasted against control PVC samples to validate the functionalization process.

1. TGA Analysis

Thermogravimetric analysis was performed on PVC and TSC-PVC membranes and presented in Figure 32. Decomposition of non-modified PVC membrane starts in the range of 240-250°C. The addition of TSC ligand to the PVC surface reduced the thermal stability of the membrane, with breakdown beginning around 240°C. Furthermore, for the same mass loss, PVC membrane degrades over a temperature range of 130°C, whereas TSC-PVC decomposes over a shorter range of 50°C. This change in thermal stability validates the substitution of chlorine atoms of the PVC fibers by an amine group (Mohy Eldin et al., 2018); with the latter coming from the modification by the TSC ligand.

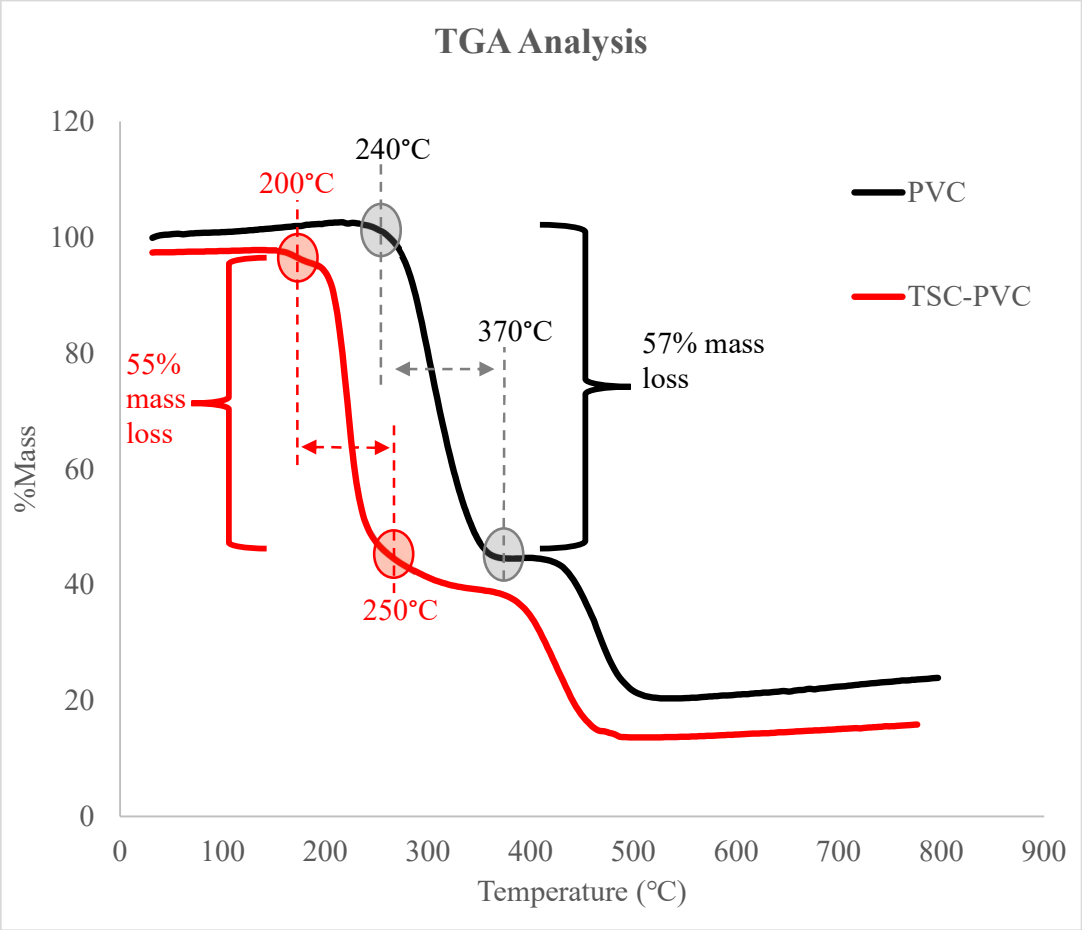

Figure 32. TGA measurements for PVC and TSC-PVC membranes

3. *Physical and Elemental Characterization: SEM and EDX Analysis*

TSC-PVC and non-modified PVC membranes were analyzed by SEM to assess the influence of the functionalization on the fibers' morphology (Figure 33). Furthermore, EDX was utilized to qualitatively confirm the elemental composition of membrane samples, namely the presence of sulfur and nitrogen; confirming the modification process. For both tests, samples were coated with a 10 nm layer of platinum.

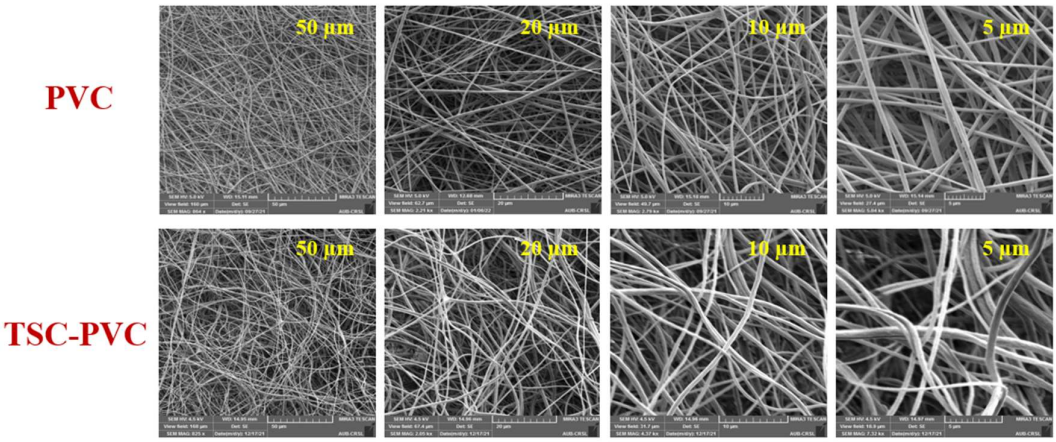

Figure 33.SEM images of PVC and TSC-PVC nanofibers

Similar to results with the TCH-PVC, SEM images of TSC-PVC illustrate that the modification had an effect on membrane morphology, with reducing the spacing between the fibers and increasing their entanglement. Again, the latter can be due to hydrogen bonding, which validates the functionalization process. Furthermore, the presence of sulfur was observed in the EDX spectra (Figure 34), validating the prior.

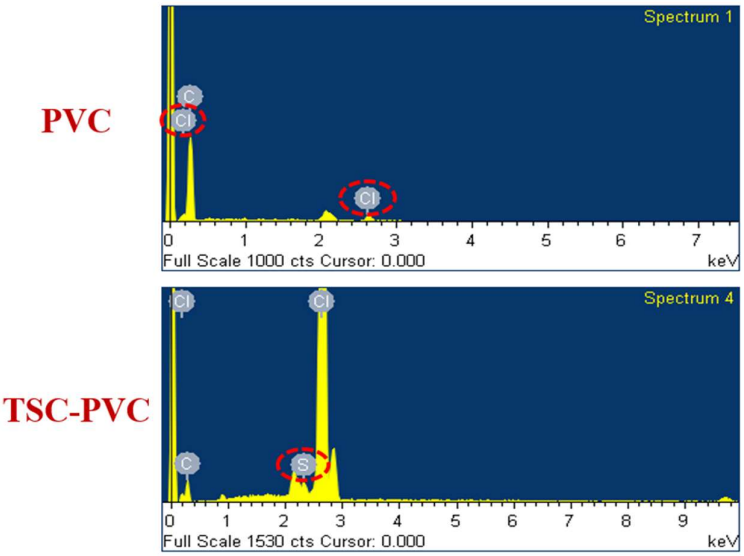

Figure 34. EDX spectra of PVC and TSC-PVC nanofibers

4. Pore Size Distribution and Water Contact Angle

The pore size distribution of the PVC membrane before and after functionalization with the TSC ligand was measured, as shown in Figure 49 in Appendix I. Similar to the results with TCH-PVC, TSC-PVC showed a smaller average pore size diameter of 2.581 µm, compared to 2.86 µm for PVC. The reduction in pore size distribution corresponds to the rise in fiber entanglement seen in the SEM investigation, which may result in increased adsorption capacity (Jamshidi Gohari et al., 2015). In addition, and as observed in the previous chapter, the bigger the electrospun membrane thickness, the smaller the pore size (Asmatulu et al., 2018). This was consistent with our findings with the TSC-PVC membrane, where the thickness of the functionalized membrane was larger than that of the PVC membrane (Table 12). Subsequently, the former had a lower average pore size than the latter.

Table 12. Thickness and pore size distribution

Parameter	**PVC**	**TSC-PVC**
Mean Pore Diameter (µm)	2.86	2.58
Average Thickness (µm)	105 ± 11	185 ± 22

In order to investigate the effect of membrane functionalization on the hydrophilicity of the membrane, the water contact angle was measured for PVC and TSC-PVC membranes (Figure 35). The functionalization of the PVC membrane had a negligible effect on the membrane hydrophilicity, as shown in Table 13. This is due to the same reason observed with the TCH-PVC; the reduction in pore size, which

increases the membrane's hydrophobicity, in combination with the hydrophilic effect of the TSC's amine groups, nullifying their effects and resulting in negligible changes in the membrane's wettability.

Figure 35. CA measurements for PVC and TSC-PVC membranes

Table 13. PVC and TSC-PVC CA results

Parameter	**PVC**	**TSC-PVC**
Range	128.0°-138.0°	112.0°-145.0°
Mean	132.6°	128.1°

D. Removal Efficiency of Heavy Metal Ions from Water

Having confirmed and characterized the functionalization process, the adsorption capability of TSC-PVC membranes was assessed towards the removal of silver(I) and mercury(II) from mono-ionic water solutions. As TSC and TCH have comparable binding patterns, and because TCH-PVC was not found to sequester Cd(II) and Pb(II) from solution, it was anticipated that the TSC-PVC membrane would not remove these metals either. As a result, TSC-PVC removal testing of Cd(II) and Pb(II) was confined to the mixed metal system described in this chapter.

3. Silver(I) Removal

The adsorption efficiency of Ag(I) using a TSC-PVC membrane was evaluated using a 100 ppm solution of Ag(I) in water. TSC-PVC membrane (20 mg) was immersed in 10 ml of silver(I) solution and shaken for 24 hours at room temperature and neutral pH at 600 rpm. Treated water samples were collected after 10 minutes, 20 minutes, 30 minutes, 1 hour, 2 hours, 3 hours, 5 hours, and 24 hours to determine removal ability using atomic absorption spectroscopy (AAS). The calibration curve presented in Figure 50 in Appendix II was utilized for this experiment.

As demonstrated in Figure 36, the TSC-PVC membrane removed 79.6% of the silver(I) from solution in 20 minutes and 97.5% after 24 hours. Unmodified PVC membranes had negligible silver removal (<1%), confirming the enhancement of silver removal from water as a result of the incorporation of the TSC ligand into the membrane fibers.

The treated membranes were then rinsed with distilled water and dried before being examined with SEM and EDX (Figure 37). The TSC-PVC membrane used in the treatment had a sensing effect compared to the unmodified PVC (Figure 37-(a) & (b)). Additionally, SEM micrographs detected silver structures on the TSC-PVC fibers which were confirmed by EDX.

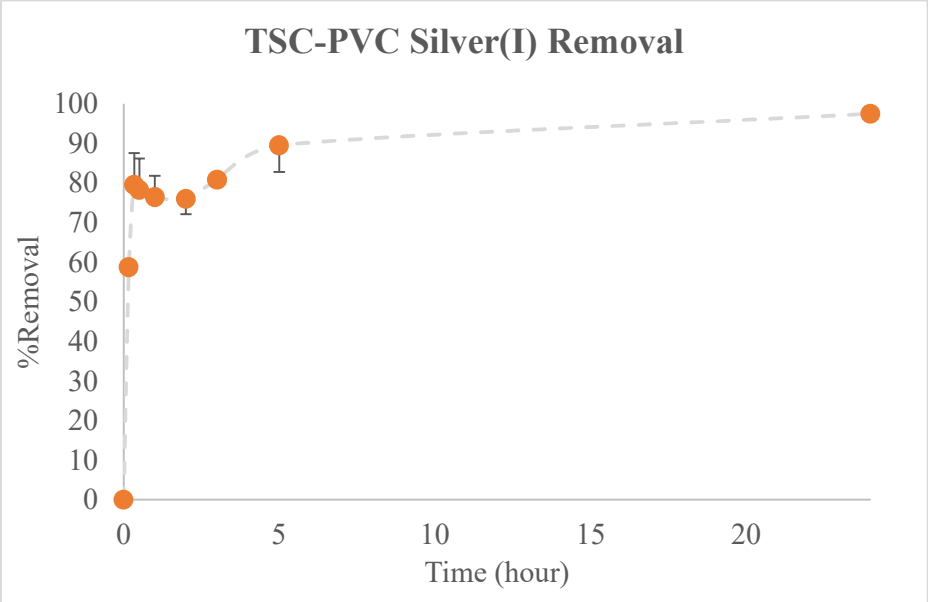

Figure 36. Percentage removal of Ag(I) from solution ([Ag]=100 ppm, at room temperature, and pH=7)

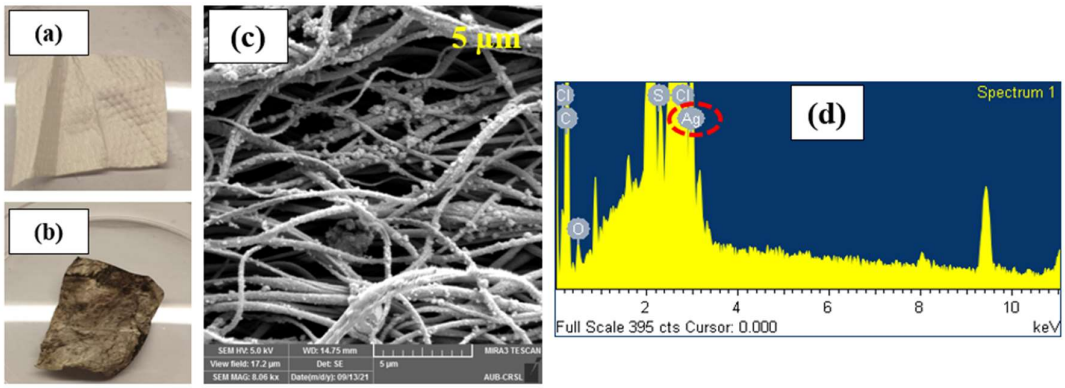

Figure 37. Physical analysis of membranes used in silver sorption (a) PVC-Ag, (b) TSC-PVC-Ag membrane sensing, (c) SEM micrograph of TSC-PVC-Ag, and (d) EDX spectra of TSC-PVC-Ag

4. Mercury(II) Removal

Similar to silver(I) removal testing, 20 mg of TSC-PVC membrane was immersed in 10 ml of a 100 ppm mercury(II) solution in water and shaken at 600 rpm

for 24 hours. The calibration curve presented in Figure 51 was utilized for this experiment.

The TSC-PVC membrane absorbed 71.6% of the mercury(II) from solution in one hour and 76.6% after 24 hours, as shown in Figure 38. Mercury removal was negligible (<3%) in unmodified PVC membranes, indicating mercury removal as a result of the incorporation of the TSC ligand into the membrane fibers, which then interacted with the metal in solution.

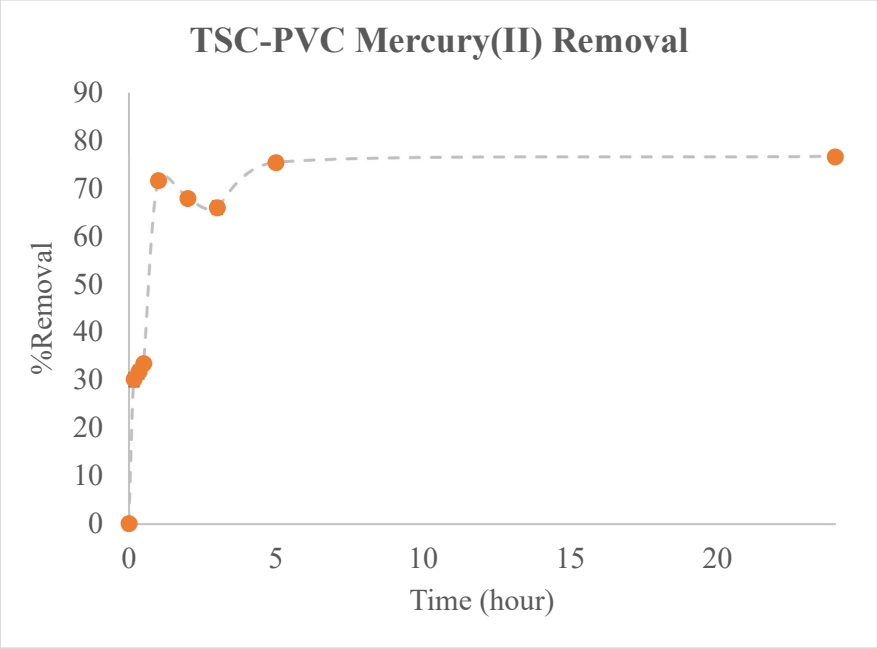

Figure 38. Percentage removal of Hg(II) from solution ([Hg]=100 ppm, at room temperature, and pH=7)

The membranes used to absorb mercury ions were similarly examined with SEM and EDX (Figure 39). The TSC-PVC membrane employed in mercury sorption displayed a sensing effect compared to the unmodified PVC (Figure 39-(a) & (b)). Furthermore, SEM images detected mercury elements on the TSC-PVC fibers which were confirmed by EDX.

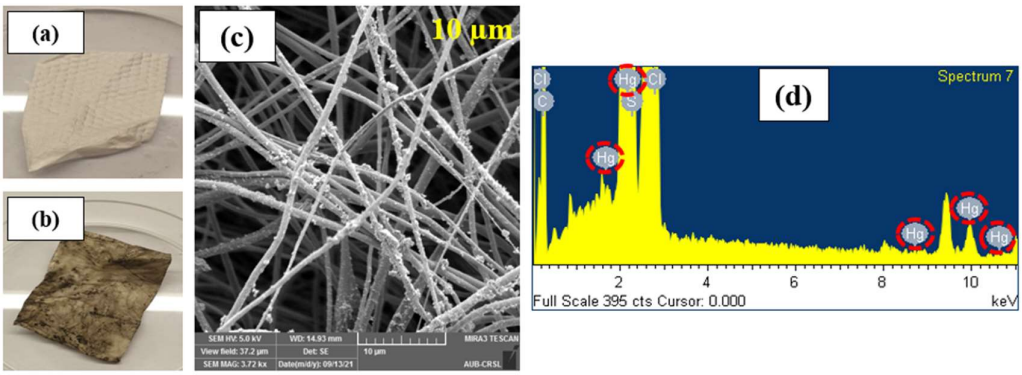

Figure 39. Physical analysis of membranes used in mercury sorption (a) PVC-Hg, (b) TSC-PVC-Hg membrane sensing, (c) SEM micrograph of TSC-PVC-Hg, and (d) EDX spectra of TSC-PVC-Hg

5. TGA Characterization of TSC-PVC Post Metals Sequestration

TSC-PVC membranes used to sequester heavy metals were subjected to thermogravimetric analysis to detect possible changes in the membranes' thermal structure, which would confirm the sorption of heavy metals onto the TSC-PVC fibers.

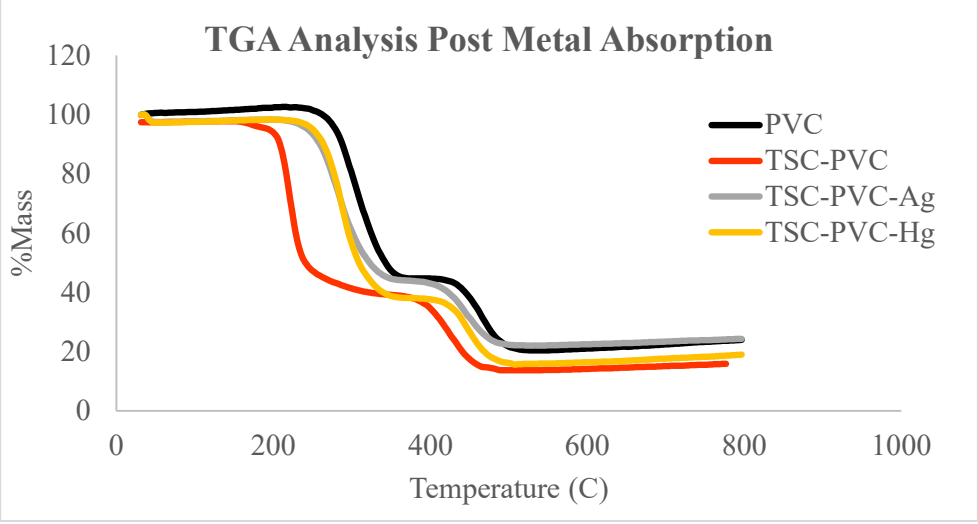

Figure 40. TGA measurements for membrane post metal absorption

As depicted in Figure 40, the membranes used in metal removal break down at higher temperatures than the TSC-PVC membrane. This discrepancy indicates that

metals were adsorbed on the surface of the TSC-PVC, and subsequently enhanced the adsorbent's structural strength and stability.

6. Adsorption Kinetics

After confirming the removal of Ag(I) and Hg(II), the effect of contact time on their absorption onto the TSC-PVC adsorbent was studied to establish the optimal uptake time from synthetic wastewater. The kinetic mechanisms of the adsorption process indicated in Figures 36 and 38 were fitted with two models; pseudo-first order (eqn. (4)) and the pseudo-second order (eqn. (5)). A strong correlation with the pseudo-first order would imply that the reaction is physisorption. However, if the reaction fits well the Pseudo second order model, it shows a proclivity for chemisorption (Wang et al., 2007).

$$\frac{1}{q_t} = \frac{k_1}{Q_1} t + \frac{1}{Q_1} \tag{4}$$

Where:

- q_t: adsorption capacity at time t (mg/g)
- Q_1: equilibrium adsorption capacity (mg/g)
- k_1: adsorption rate constant of pseudo-first order (min^{-1})

$$\frac{t}{q_t} = \frac{t}{q_e} t + \frac{1}{k_2 q_e^2} \tag{5}$$

Where:

- q_e: amount of metal adsorbed at equilibrium (mg/g)
- k_2: equilibrium rate constant of pseudo-second order ($\frac{g}{mg.min}$)

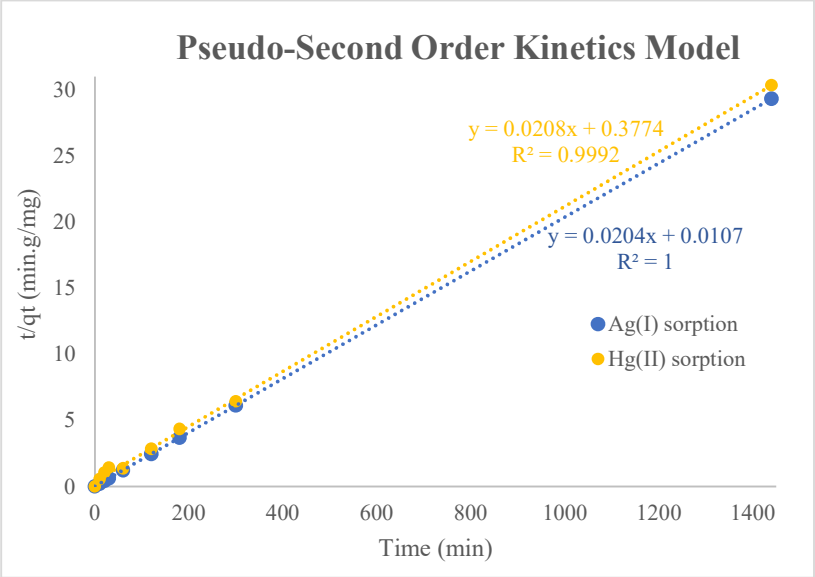

Figure 41. Pseudo-second order kinetics model

As demonstrated in Figure 41, the pseudo-second order model can predict silver adsorption kinetics with a coefficient of determination of 100%, whereas the coefficient of determination of the pseudo-first order model was significantly low (19.5%) (Figure 54 in Appendix III). Similarly, the mercury adsorption kinetics is guided by a pseudo-second order model with a coefficient of determination of 99.92%.

As the pseudo-second order adsorption process is assumed to occur as a result of a primarily chemical reaction. This validates the study's foundation, which is the chemical chelation of heavy metal ions via the creation of coordination bonds with the ligands. Table 14 summarizes the pseudo-second order adsorption characteristics for each metal. The equilibrium capacity and reaction rate for Ag(I) sorption are greater than those for Hg(II), supporting the experimental findings of a faster and higher absorption of Ag(I) by TSC-PVC.

Table 14. Adsorption kinetics model parameters

Parameter	**Silver(I)**	**Mercury(II)**
q_e *(mg/g)*	49.02	48.08
k_2 $(\frac{g}{mg.min})$	3.89×10^{-2}	1.14×10^{-3}

7. Adsorption Isotherms

To evaluate the interaction with the TSC-PVC adsorbent, adsorption equilibrium testing was performed with varied starting concentrations of Ag(I) and Hg(II) of 50, 100, 150, 200, 250, 300, and 350 ppm while keeping the concentration of the membrane constant. TSC-PVC membranes (10 mg) were added to 5 ml of each prepared solution containing different concentrations of each metal and shaken at room temperature and neutral pH. Treated water was sampled at the conclusion of the 24 hours period and analyzed for metal removal by AAS. The amount of adsorbed metal ions at equilibrium q_e (mg/g) was calculated using eqn. (6):

$$q_e = \frac{C_i - C_f}{W} v \qquad (6)$$

Where:

- C_i: initial metal concentration (mg/g)
- C_f: equilibrium metal concentration (mg/g)
- W: mass of TSC-PVC adsorbent used (mg)
- v: volume of solution (ml)

The experimental data were fitted using the two commonly assessed adsorption isotherm models, Langmuir and Freundlich. These models are used to represent the distribution of the adsorbent (TSC-PVC) and adsorbate (heavy metal ions) in aqueous

solutions, taking into account the adsorbent's heterogeneity/homogeneity and the interaction between the adsorbate species (Khayyun & Mseer, 2019). The Langmuir model (eqn. (7)) validates the TSC-PVC adsorbent's monolayer interaction with the metal adsorbate.

$$\frac{C_e}{q_e} = \frac{C_e}{q_{max}} + \frac{1}{q_{max} K_L} \quad (7)$$

Where:

- C_e: concentration of metal ions in solution at equilibrium (mg/l)
- q_{max}: maximum adsorption capacity (mg/g)
- K_L: Langmuir adsorption constant related to the energy of adsorption (l/mg)

The Langmuir adsorption constant is defined using eqn. (8):

$$R_L = \frac{1}{1 + C_0 K_L} \quad (8)$$

Where the separation factor R_L is a dimensionless constant, also referred to as the equilibrium parameter. As indicated in Table 15, the value of the equilibrium parameter reflects the reaction isotherms.

Table 15. Langmuir model isotherm types (Langmuir, 1918)

R_L	Isotherm Type
>1	unfavorable
$= 1$	linear
0< R_L<1	favorable
=0	irreversible

The Freundlich model is particularly useful for modeling the isotherm for heterogeneous surfaces, and it is represented by the following relationship:

$$\log(q_e) = \log(K_f) + \frac{1}{n}\log(C_e) \quad (9)$$

Where:

- K_f: sorption capacity
- $\frac{1}{n}$: sorption intensity

The sorption capacity and intensity of the Freundlich model are calculated using the linear regression slope and intercept. As indicated in Table 16, the value of n represents the type of isotherm:

Table 16. Freundlich model isotherm types (Freundlich, 1906)

1/n	**Isotherm Type**
>1	unfavorable
0< R_L<1	favorable
=0	irreversible

Langmuir modeling of Ag(I) and Hg(II) sorption (Figure 42) yielded a high coefficient of determination (over 99% for both metals sorption). The Freundlich models (Figure 43) produced a low linear correlation. This demonstrates that the adsorption behavior of Ag(I) and Hg(II) over the TSC-PVC membrane follows the Langmuir model; following a monolayer chemical sorption process.

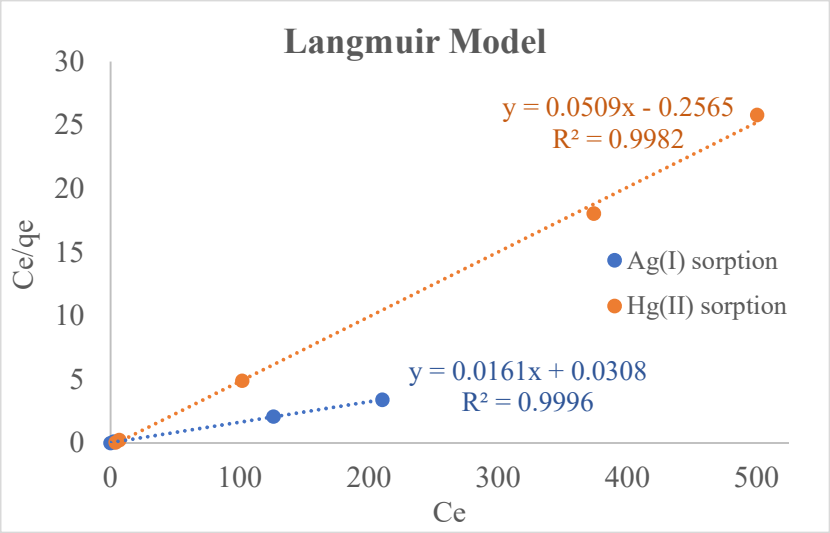

Figure 42. Amount of heavy metal removal from solution by Langmuir model

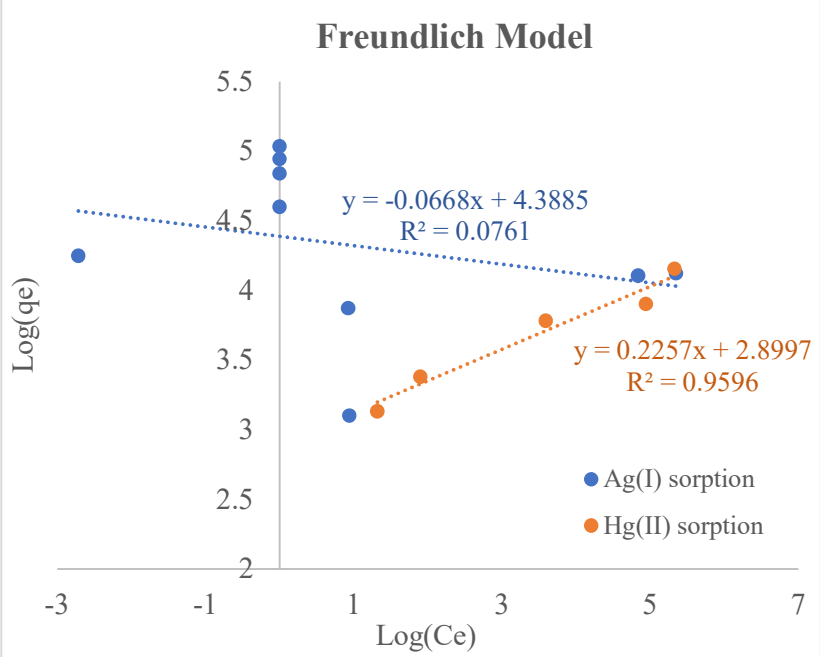

Figure 43. Amount of heavy metal removal from solution by Freundlich model

The maximum adsorption capacity (q_{max}) was determined using Langmuir modeling (eqn. (7)) and found to be 62.1 mg/g for Ag(I) sorption and 20.0 mg/g for Hg(II) sorption (Table 17). The highest absorption capacities are comparable to those

observed in the literature (Table 2), although they are not competitive with the absorption capacity produced by modified MOFs, which demonstrated a Hg(II) absorption capacity of 1667 mg/g (Jaafar et al., 2021). Despite the lack of competitive adsorption capabilities, one of the primary objectives of this study is the simple preparation and modification of electrospun membranes, which is not the case in the synthesis of MOFs

Furthermore, the separation factor (RL) for Ag(I) and Hg(II) adsorption was calculated and found to be 3.67×10^{-2} and 4.88×10^{-3} respectively. The presence of R_L values ranging from 0 to 1 for both metal adsorption processes indicates that the heavy metal ion adsorption process into TSC-PVC is a favorable interaction (Table 17).

Table 17. Metal adsorption parameter by Langmuir model

Parameter	**Silver(I)**	**Mercury(II)**
q_{max} *(mg/g)*	62.1	20.0
K_L	0.52	0.20
R_L	3.67×10^{-2}	4.88×10^{-3}

8. Ion Selectivity

The TSC-PVC membrane demonstrated a capacity for Ag(I) and Hg(II) uptake in monoionic water solutions. However, industrial wastewater frequently combines a variety of metal ions, which may affect the TSC-PVC membrane's removal capacity. As a result, the TSC-PVC membrane's sorption effectiveness was investigated in a mixed metal system including 100 ppm of Ag(I), Hg(II), Cd(II), Pb(II), Cu(II), and Zn(II). The solution was shaken for 24 hours at ambient temperature and neutral pH. The sorption

efficiency (removal percentage) for each metal by the TSC-PVC membrane was evaluated using AAS as illustrated in Figure 44.

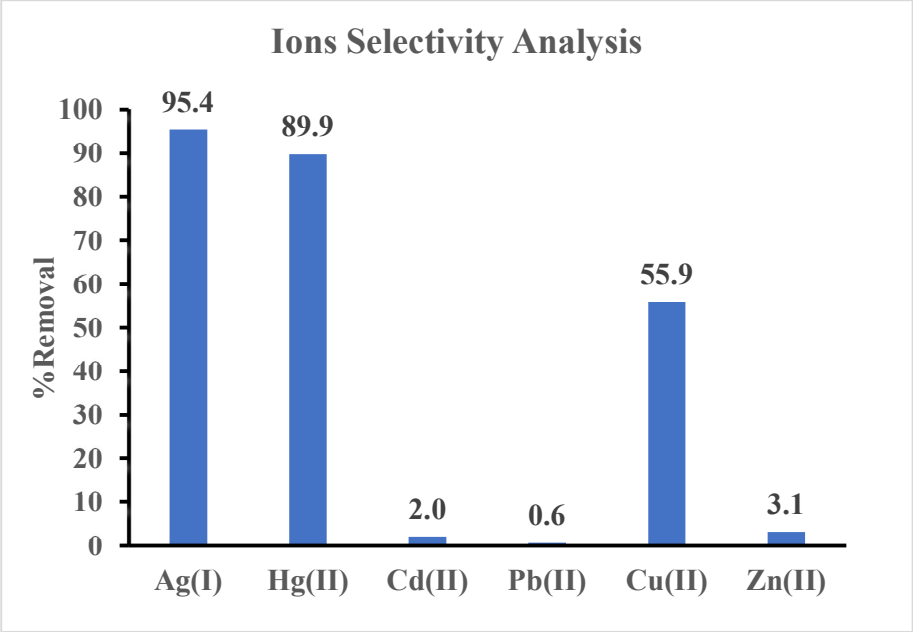

Figure 44. Ion selectivity analysis

As demonstrated in Figure 44, the removal efficacy of the TSC-PVC membrane towards Ag(I) and Hg(II) metals was largely unaffected by the presence of competing ions, demonstrating the functionalized membrane's adsorption selectivity towards Ag(I) and Hg(II), respectively. This could be attributed to the electron donor groups of the TSC ligand, namely sulfur. Silver and mercury are well known to be highly thiophilic (Wang et al., 2020; Melnick et al., 2010); having a high affinity for sulfur in its various forms. As a result, TSC-PVC membranes have the ability to efficiently sequester Ag(I) and Hg(II) metal ions from industrial effluent.

9. Regeneration of TSC-PVC membranes

This study was conducted in order to produce a green and sustainable approach to water purification; to create a system that can be reused with low energy input and waste generation. This was accomplished by testing the TSC-PVC membrane for recyclability of removing Ag(I) and Hg(II) metals from mono-ionic solutions.

Sequential adsorption-desorption studies were carried out for five cycles at an initial concentration of 100 ppm to assess the repeated use of the modified nanofiber membranes in metal adsorption. TSC-PVC membranes were regenerated at the conclusion of each adsorption experiment with a 0.1 M *p*-toluene sulfonic acid solution at a pH of 5.5. The coordination bonds between the TSC ligand and the metal ions are disintegrated by this acidic solution (Li et al., 2021). The performance of the regenerated TSC-PVC membrane for Ag(I) and Hg(II) removal, respectively, is illustrated in Figures 45 and 46.

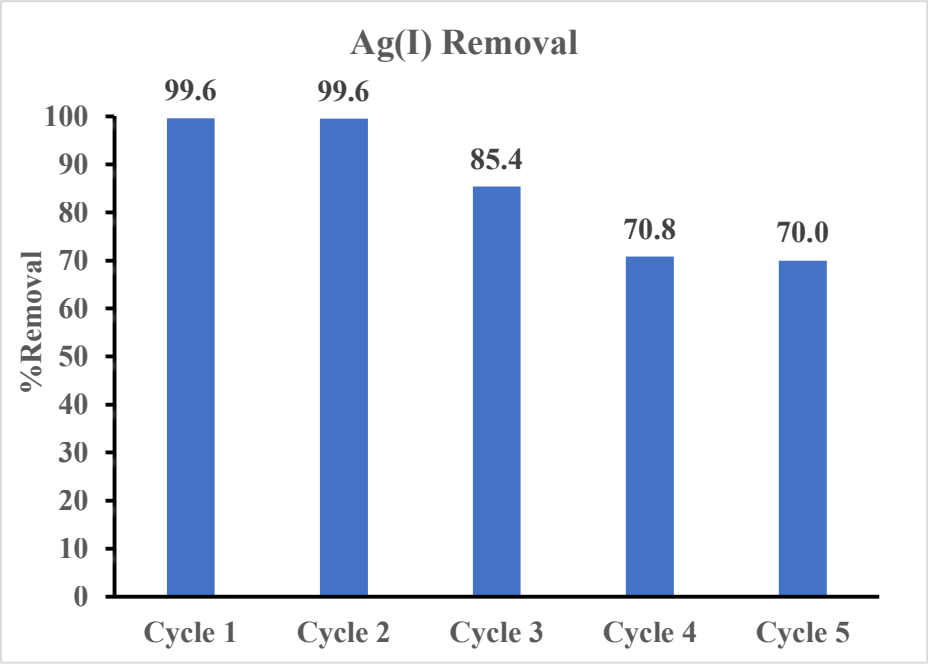

Figure 45. Recyclability of TSC-PVC for the removal of Ag(I) ions ([Ag(I)]=100 ppm)

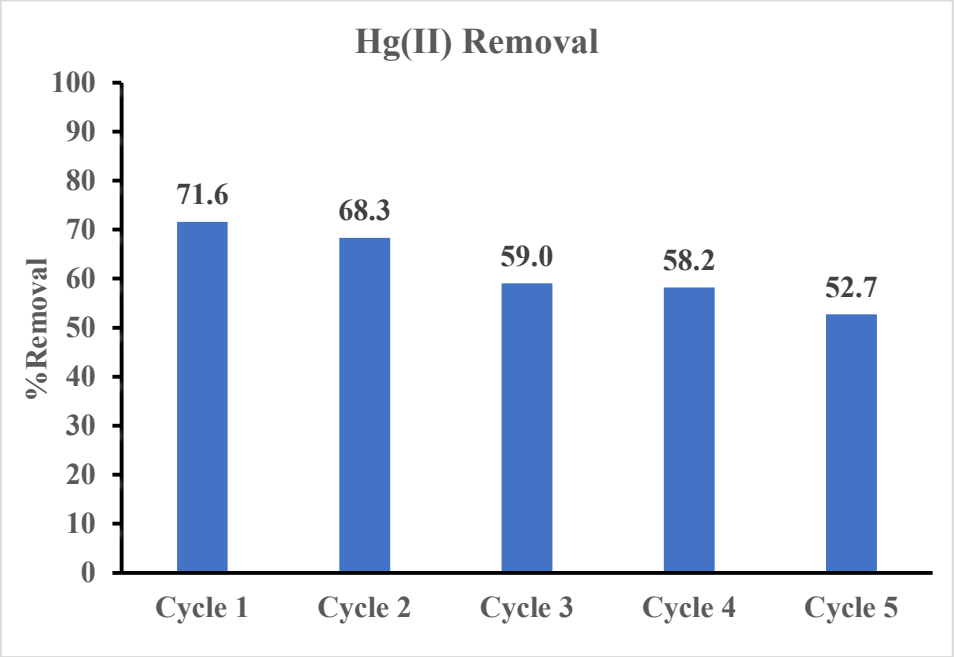

Figure 46. Recyclability of TSC-PVC for the removal of Hg(II) ions ([Hg(II)]=100 ppm)

The sorption efficiency of TSC-PVC Ag(I) does not decline substantially until the third cycle, as illustrated in Figure 45. In the initial adsorption trial, the efficacy of Ag(I) removal was reduced by 0.07% after the first cycle compared to the unused membranes, and by 14% after the second cycle. The removal efficiency of Ag(I) remained constant at 70% after the third cycle for two more cycles.

Similarly, as shown in Figure 46, the TSC-PVC Hg(II) uptake effectiveness remains relatively constant over cycles 1 and 2. The removal effectiveness declines by 9.3% at the end of the second cycle and remains steady at approximately 59% for two cycles before further deterioration by the end of the fourth cycle.

Evidently, the TSC-PVC membrane can be effectively reused for Ag(I) and Hg(II) removal for three cycles with substantial efficiency and subsequent removal cycles with declining sorption.

Furthermore, SEM examination of the regenerated membranes confirms the absence of metal elements from the nanofibers following desorption, followed by their reappearance in subsequent adsorption cycles (Figure 47).

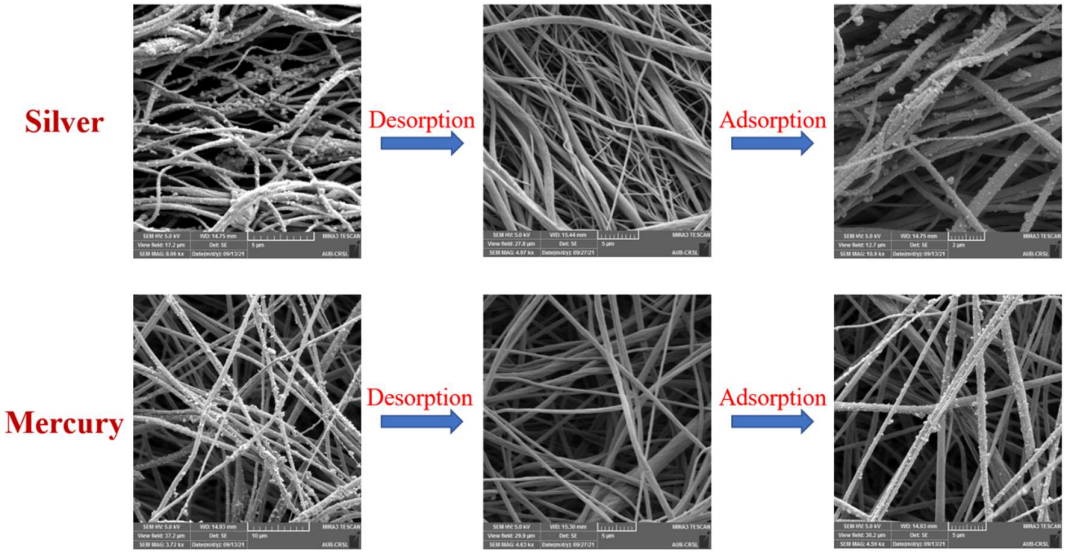

Figure 47. SEM images of TSC-PVC throughout regeneration cycles

The degradation in removal capacity demonstrates that in the acidic medium of the regeneration step, functional groups of the TSC ligand (particularly sulfur) became partially protonated, and the adsorbed metal ions on these groups were replaced by H^+ ions. As surface charges accumulated over regeneration cycles, repulsion between protonated sites and metal cations in adsorption increased, resulting in a drop in removal efficiency (Wang et al., 2013; Meng et al., 2018). Other variables, such as incomplete acid treatment and the likelihood of irreversible interaction of active sites on the TSC ligand with metal cations, might have also contributed to the observed deterioration in removal efficiency (Hezarjaribi et al., 2021).

E. Comparative Analysis of TCH-PVC and TSC-PVC

Having synthesized, characterized, and analyzed the metal sorption efficiencies of the two modified TCH-PVC and TSC-PVC membranes, their experimental results are contrasted in Table 18. TCH and TSC ligands have comparable stability constants with Ag(I), as shown in Table 18, whereas TCH demonstrated greater binding with Hg(II) ions. However, the latter did not result in improved Hg(II) sorption by TCH-PVC, owing to the fact that TCH-PVC has a different binding motif with Hg(II) than with TCH separately, as discussed in Chapter I.

Table 18. Comparative analysis of TCH-PVC and TSC-PVC adsorbents

Parameter	**TCH-PVC**	**TSC-PVC**
Ag(I)-Ligand Stability Constant $[M^{-1}]$	2.6×10^3	4.2×10^3
Hg(II)-Ligand Stability Constant $[M^{-1}]$	1.13×10^7	3.2×10^4
PVC:Ligand Preparation Ratio	1:5	1:3
PVC:Ligand Degree of Modification	$1{:}1.3 \pm 0.2$	$1{:}0.5 \pm 0.15$
Water Contact Angle	132.5°	128.1°
Mean Pore Diameter (µm)	2.79	2.58
Average Thickness (µm)	196 ± 13	185 ± 22
Ag(I) Sorption Efficiency	40.0%	70.3%
Hg(II) Sorption Efficiency	97.5%	76.6%

Furthermore, the hydrophobicity, membrane thickness, and mean pore diameter of both modified membranes are comparable. The enhanced Ag(I) and Hg(II) sorption with a lower PVC:ligand preparation ratio demonstrates the superiority of the TSC-PVC

adsorbent over TCH-PVC. This shows a cost benefit in the production of the TSC-PVC membrane, while also attaining improved heavy metal removal from solution.

CHAPTER VI

CONCLUSION AND RECOMMENDATION

Water pollution is a global issue that threatens the entire environment and affects the lives of millions of people worldwide. Water pollution is not only one of the leading global risk factors for illness, disease, and death; it also adds to the ongoing loss of accessible potable water globally. Providing efficient, simple to deploy, and economical solutions for water treatment is an ongoing challenge. Adsorption was established to be an effective water purification approach due to its high removal efficiency, reversibility, and capacity to regenerate and reuse adsorbents, as well as its flexible design and operation.

The development of modified polymeric electrospun nanofibers as adsorbents of heavy metal ions from water under ambient conditions was explored in this study. To improve its uptake capacity, a polyvinyl chloride (PVC) membrane was electrospun and then modified with TCH/TSC organic ligands. The structural and chemical changes induced by the modification were characterized, demonstrating that the functionalization of the membranes was achieved.

Prior to testing the adsorption capabilities of the modified membranes, the interaction of the organic ligands with the tested metals was evaluated in solution in the absence of the membranes. Titration experiments indicated that TCH and TSC ligands form complexes with silver(I) and mercury(II). The integration of these ligands on the PVC surface considerably improved metal removal relative to the unmodified PVC membrane. The TCH-PVC membrane enhanced silver(I) removal by 40% and mercury(II) removal by 70%, whereas the TSC-PVC membrane improved removal by

up to 97.5 % of silver(I) and 76.6 % of mercury(II). With a maximum adsorption capacity of 62.1 mg/g for silver(I) and 20.0 mg/g for mercury(II) by the TSC-PVC membrane, the metal removal kinetics followed the pseudo-second order and the Langmuir isotherm model. In a mixed metal system of competing metal ions, the TSC-PVC membrane also demonstrated strong chelation selectivity towards silver(I) and mercury(II) ions. Furthermore, the TSC-PVC membrane was evaluated for regeneration, yielding high sorption efficiency for three adsorption/desorption cycles and substantial absorption for two further cycles.

This work expands on the TCH/TSC ligands' known metal chelation properties, which were primarily focused on anti-bacterial activities, and investigates their effective inclusion in nanofiltration applications. Although both fabricated modified membranes were presented as efficient materials for heavy metal ion decontamination in this study, TSC-PVC membranes are more efficient materials in heavy metal ion removal than TCH-PVC, owing to the former fibers' better adsorption capacities in removing silver(I) and mercury(II). Although the achieved adsorption capacities are not superior to those of other emerging technologies, the latter would need a more complex synthesis and more expensive operation, namely in the preparation of adsorption conditions (temperature and pH). The methods proposed in this study are appropriate for water treatment applications that need simplicity, low cost, and appropriate for use at ambient temperature and neutral pH.

The efficiency of the fabricated membranes in the removal of metals at larger scale industrial wastewater, which was replicated in the laboratory mixed metal system in this study, might be examined further in future work. Furthermore, expanding the pool and altering the amounts of competing metal cations should be investigated.

Additionally, while the goal of this work was to produce a simple removal system under ambient circumstances, the influence of pH change on the sorption effectiveness of the membranes should be investigated in order to imitate real wastewater rich in salts. Importantly, the functionalization in this work was accomplished by a chemical modification of the membrane's surface. It is suggested that the organic ligands be incorporated into the PVC matrix and that the resulting electrospun membrane be evaluated for removal behavior.

APPENDIX I: MEMBRANE PORE SIZE DISTRIBUTION

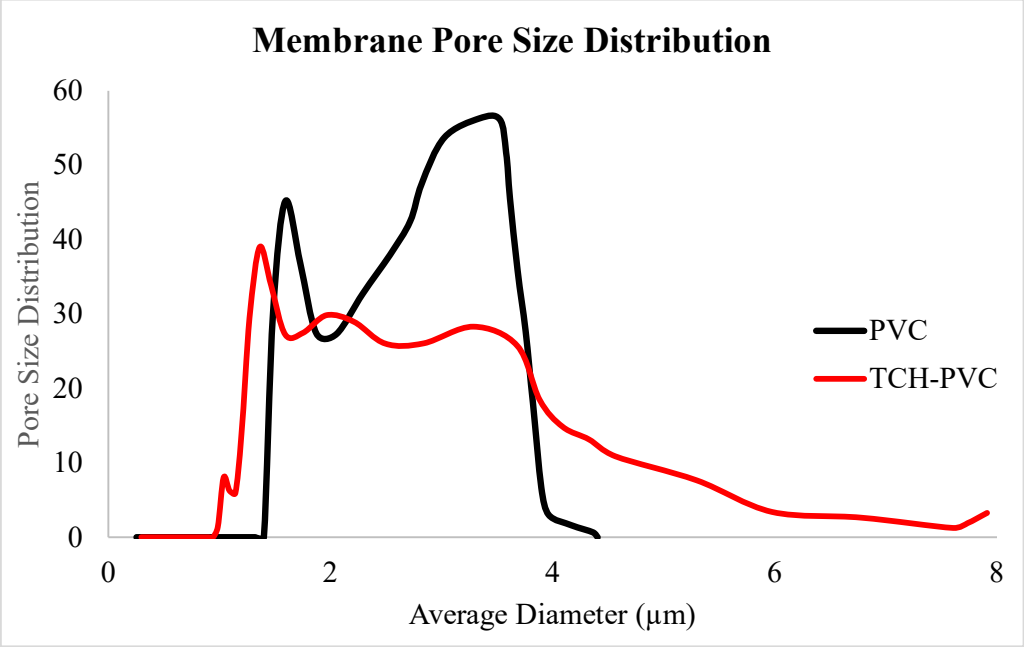

Figure 48. PVC and TCH-PVC membrane pore size distribution

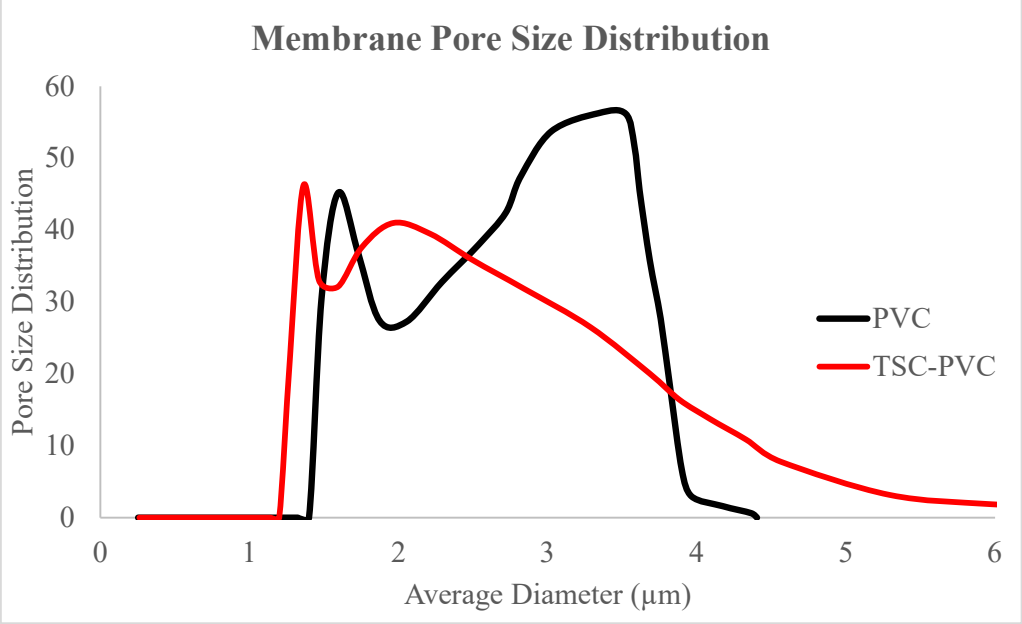

Figure 49. PVC and TSC-PVC membrane pore size distribution

APPENDIX II: AAS CALIBRATION CURVES

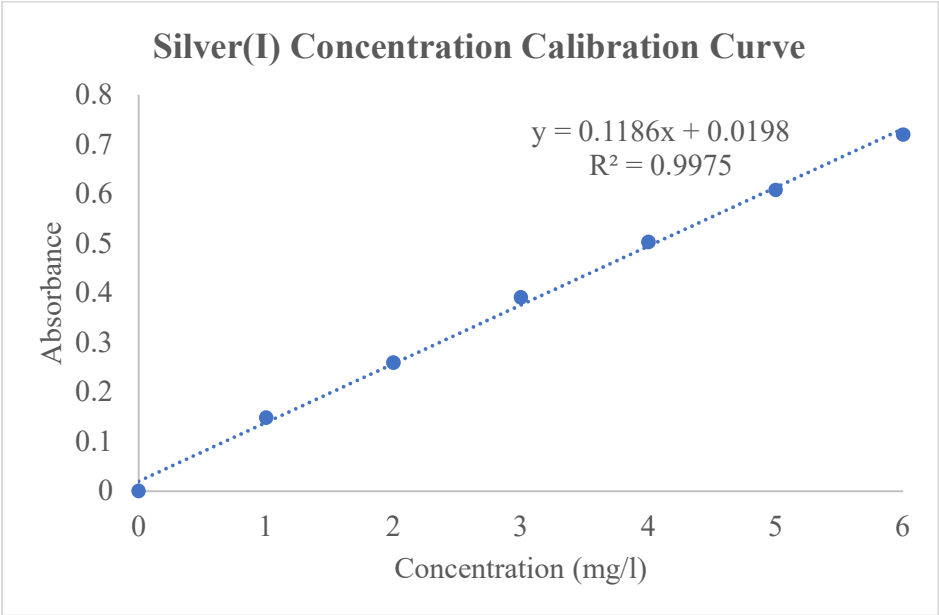

Figure 50. Calibration curve for silver(I) concentration

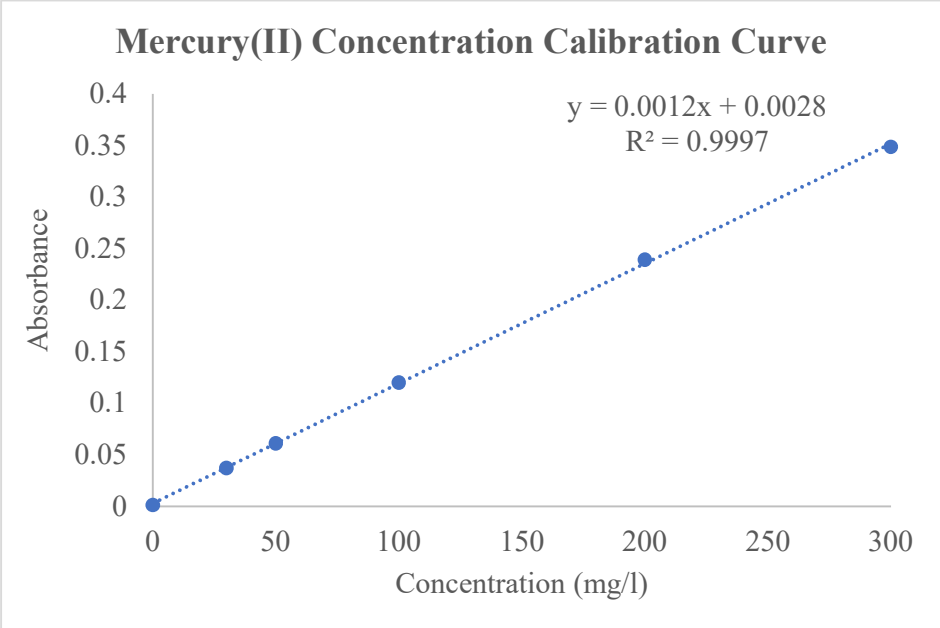

Figure 51. Calibration curve for mercury(II) concentration

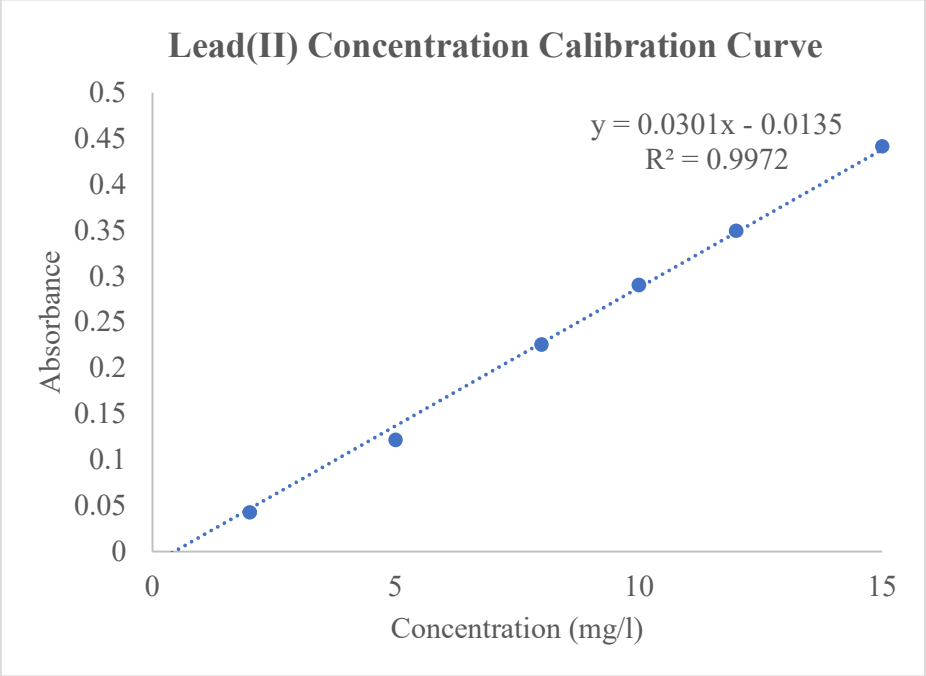

Figure 52. Calibration curve for lead(II) concentration

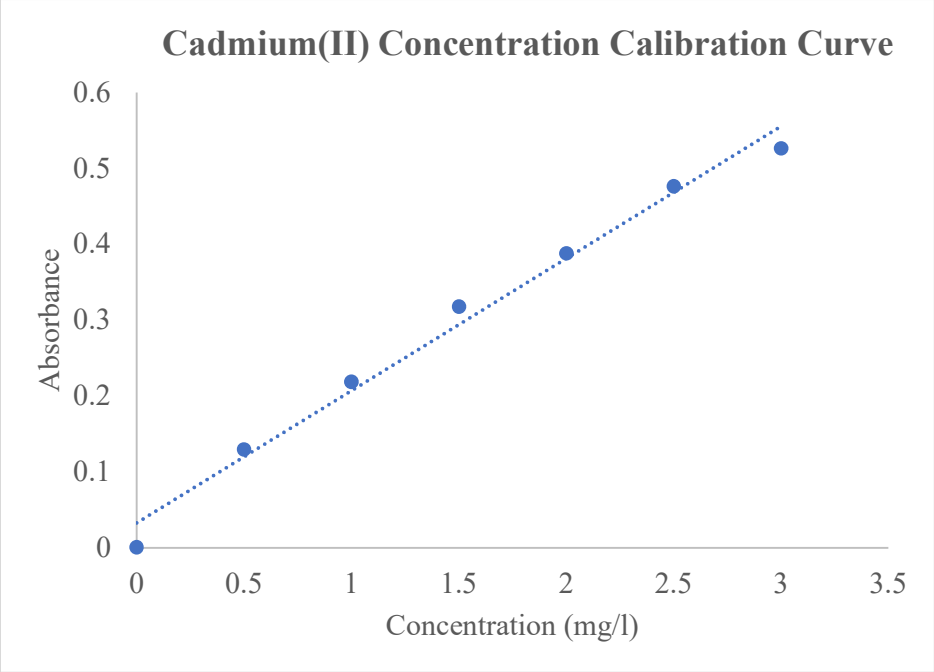

Figure 53. Calibration curve for cadmium(II) concentration

APPENDIX III: PSEUDO-FIRST ORDER KINETICS MODEL

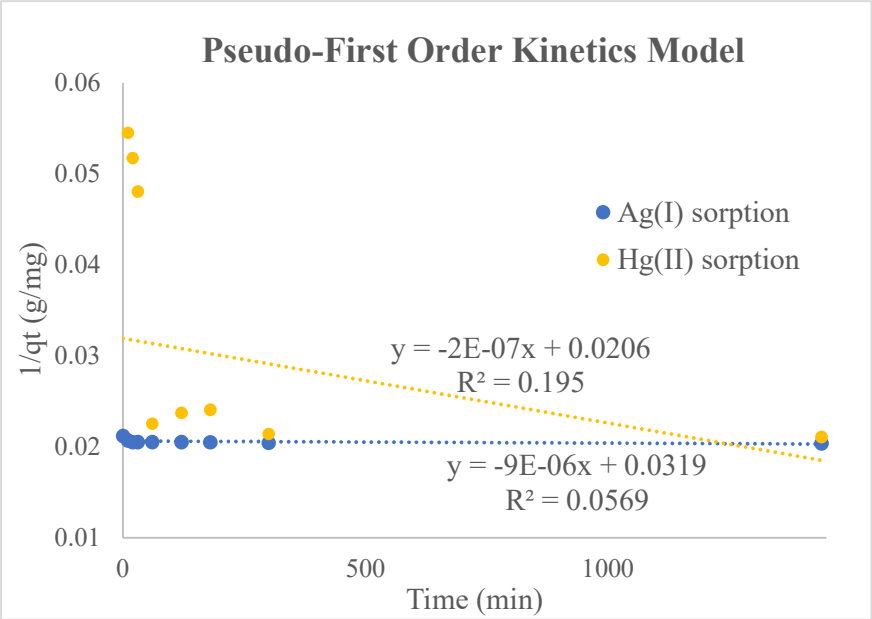

Figure 54. Pseudo-first order kinetics model

REFERENCES

Abu-Hussen, A. A. A., & Emara, A. A. A. (2004). Metal complexes of some thiocarbohydrazone ligands: Synthesis and structure. *Journal of Coordination Chemistry, 57*(11), 973-987. https://doi.org/10.1080/00958970412331272412

Ajiboye, T. O., Oyewo, O. A., & Onwudiwe, D. C. (2021). Simultaneous removal of organics and heavy metals from industrial wastewater: A review. *Chemosphere (Oxford)*, 262, 128379-128379. https://doi.org/10.1016/j.chemosphere.2020.128379

Ali, I., Asim, M., & Khan, T. A. (2012). Low cost adsorbents for the removal of organic pollutants from wastewater. *Journal of Environmental Management, 113*, 170-183. https://doi.org/10.1016/j.jenvman.2012.08.028

Ali, M.A. and Livingstone, S.E. (1974). Coord. Chem. Rev. 13, 279.

Almasian, A., Giahi, M., Chizari Fard, G., Dehdast, S., & Maleknia, L. (2018). Removal of heavy metal ions by MODIFIED Pan/pani-nylon CORE-SHELL NANOFIBERS Membrane: Filtration performance, antifouling and regeneration behavior. *Chemical Engineering Journal, 351*, 1166-1178. doi:10.1016/j.cej.2018.06.127

Ariaratnam, S. T., & Chammout, B. (2021). Underground space development resulting from increased urban migration. *Global Journal of Engineering and Technology Advances*, *8*(2), 046–055. https://doi.org/10.30574/gjeta.2021.8.2.0093

Asmatulu, R., Muppalla, H., Veisi, Z., Khan, W. S., Asaduzzaman, A., & Nuraje, N. (2013). Study of hydrophilic electrospun nanofiber membranes for filtration of micro and nanosize suspended particles. *Membranes (Basel), 3*(4), 375-388. https://doi.org/10.3390/membranes3040375

Asmatulu, R., S, K., Waseem, & Khan, W. S. (2018). *Synthesis and applications of electrospun nanofibers*. Elsevier. https://doi.org/10.1016/C2017-0-00516-5

Bacchi, A., Carcelli, M., Pelagatti, P., Pelizzi, C., Pelizzi, G. and Zani, F. (1999). J. Inorg. Biochem. 75, 123.

Badran, R. A. (2019). Surface modification of electrospun poly(vinyl chloride) membrane for oil-water separatioN [Master's Thesis, American University of Beirut]. AUB ScholarWorks. https://scholarworks.aub.edu.lb/handle/10938/23084

Baird, C., & Cann, M. C. (2012). *Environmental chemistry*.

Beckers, F., & Rinklebe, J. (2017). Cycling of mercury in the environment: Sources, fate, and human health implications: A review. *Critical Reviews in Environmental*

Science and Technology, 47(9), 693-794. https://doi.org/10.1080/10643389.2017.1326277

Benesi, H. A., & Hildebrand, J. H. (1949). A spectrophotometric investigation of the interaction of iodine with aromatic hydrocarbons. *Journal of the American Chemical Society, 71*(8), 2703-2707. https://doi.org/10.1021/ja01176a030

Bhatnagar, A., Sillanpää, M., & Witek-Krowiak, A. (2015). Agricultural waste peels as versatile biomass for water purification – A review. *Chemical Engineering Journal (Lausanne, Switzerland : 1996), 270*, 244-271. https://doi.org/10.1016/j.cej.2015.01.135

Bralower , T., & Bice, D. (2022). *Distribution of water on the Earth's surface*. Distribution of Water on the Earth's Surface | EARTH 103: Earth in the Future. Retrieved March 1, 2022, from https://www.e-education.psu.edu/earth103/node/701

Buxbaum, G. & Pfaff, G. (2005). Cadmium Pigments. *Industrial inorganic pigments* (pp. 121-123). Wiley-VCH. ISBN 978-3-527-30363-2.

Cesário, R., Hintelmann, H., Mendes, R., Eckey, K., Dimock, B., Araújo, B., Mota, A. M., & Canário, J. (2017). Evaluation of mercury methylation and methylmercury demethylation rates in vegetated and non-vegetated saltmarsh sediments from two portuguese estuaries. *Environmental Pollution (1987), 226*, 297-307. https://doi.org/10.1016/j.envpol.2017.03.075

Chang, C., Yin, R., Zhang, H., & Yao, L. (2019). Bioaccumulation and health risk assessment of heavy metals in the Soil–Rice system in a typical seleniferous area in central china. *Environmental Toxicology and Chemistry, 38*(7), 1577-1584. https://doi.org/10.1002/etc.4443

Cheng, H., Li, Z., Huang, Y., Liu, L., & Wu, H. (2017). Pillararene-based aggregation-induced-emission-active supramolecular system for simultaneous detection and removal of mercury(II) in water. *ACS Applied Materials & Interfaces, 9*(13), 11889-11894. https://doi.org/10.1021/acsami.7b00363

Crawford, C. B., & Quinn, B. (2017). The interactions of microplastics and chemical pollutants. *Microplastic Pollutants,* 131-157. doi:10.1016/b978-0-12-809406-8.00006-2

Dai, X. J., Plessis, J. d., Kyratzis, I. L., Maurdev, G., Huson, M. G., & Coombs, C. (2009). Controlled amine functionalization and hydrophilicity of a poly(lactic acid) fabric. *Plasma Processes and Polymers, 6*(8), 490-497. https://doi.org/10.1002/ppap.200800216

Das, S., & Dash, H. R. (2017). Handbook of metal-microbe interactions and bioremediation. CRC Press. https://doi.org/10.1201/9781315153353

De Gisi, S., Lofrano, G., Grassi, M., & Notarnicola, M. (2016). Characteristics and adsorption capacities of low-cost sorbents for wastewater treatment: A review. Sustainable Materials and Technologies, 9, 10-40. https://doi.org/10.1016/j.susmat.2016.06.002

Deitzel, J. M., Kleinmeyer, J., Harris, D., & Beck Tan, N. C. (2001). The effect of processing variables on the morphology of electrospun nanofibers and textiles. *Polymer (Guilford), 42*(1), 261-272. https://doi.org/10.1016/S0032-3861(00)00250-0

Drake, P. L., & Hazelwood, K. J. (2005). Exposure-related health effects of silver and silver compounds: A review. *The Annals of Occupational Hygiene, 49*(7), 575-585. https://doi.org/10.1093/annhyg/mei019

Emara, A.A.A., Khalil S.M.E., and Salib, K.A.R. (1995). J. Coord. Chem. 36, 289.

Feng, C., Khulbe, K. C., Matsuura, T., Tabe, S., & Ismail, A. F. (2013). Preparation and characterization of electro-spun nanofiber membranes and their possible applications in water treatment. *Separation and Purification Technology, 102*, 118-135. https://doi.org/10.1016/j.seppur.2012.09.037

Feng, Q., Wu, D., Zhao, Y., Wei, A., Wei, Q., & Fong, H. (2018). Electrospun AOPAN/RC BLEND nanofiber membrane for EFFICIENT removal of heavy metal ions from water. *Journal of Hazardous Materials, 344*, 819-828. doi:10.1016/j.jhazmat.2017.11.035

Feo, G. D., & Gisi, S. D. (2014). Using MCDA and GIS for hazardous waste landfill siting considering land scarcity for waste disposal. Waste Management (Elmsford), 34(11), 2225-2238. https://doi.org/10.1016/j.wasman.2014.05.028

Figueiredo, N. L., Canário, J., Serralheiro, M. L., & Carvalho, C. (2017). Optimization of microbial detoxification for an aquatic mercury-contaminated environment. *Journal of Toxicology and Environmental Health, Part A: 3rd International Conference on Occupational & Environmental Toxicology/3rd Ibero-American Meeting on Toxicology and Environmental Health International, 21-23 June 2016, Porto, Portugal, 80*(13-15), 788-796. https://doi.org/10.1080/15287394.2017.1357311

Freundlich, H. (1906). Adsorption in Solutions. *Journal of Physical Chemistry, 57*, 384-410.

Fu, F., & Wang, Q. (2011). Removal of heavy metal ions from wastewaters: A review. Journal of Environmental Management, 92(3), 407-418. https://doi.org/10.1016/j.jenvman.2010.11.011

Gall, J. E., Boyd, R. S., & Rajakaruna, N. (2015). Transfer of heavy metals through terrestrial food webs: A review. *Environmental Monitoring and Assessment, 187*(4), 1-21. https://doi.org/10.1007/s10661-015-4436-3

Gao, J., Qin, Y., Zhou, T., Cao, D., Xu, P., Hochstetter, D., & Wang, Y. (2013). Adsorption of methylene blue Onto activated carbon produced from tea (CAMELLIA Sinensis L.) SEED shells: Kinetics, equilibrium, and thermodynamics studies. *Journal of Zhejiang University SCIENCE B, 14*(7), 650-658. doi:10.1631/jzus.b12a0225

Gao, J., Sun, S., Zhu, W., & Chung, T. (2014). Chelating polymer modified P84 nanofiltration (NF) hollow fiber membranes for high efficient heavy metal removal. *Water Research (Oxford), 63*, 252-261. https://doi.org/10.1016/j.watres.2014.06.006

Gao, R., Bonin, L., Arroyo, J. M. C., Logan, B. E., & Rabaey, K. (2021). Separation and recovery of ammonium from industrial wastewater containing methanol using copper hexacyanoferrate (CuHCF) electrodes. *Water Research (Oxford)*, 188, 116532. https://doi.org/10.1016/j.watres.2020.116532

Gautam, R. K., Mudhoo, A., Lofrano, G., & Chattopadhyaya, M. C. (2014). Biomass-derived biosorbents for metal ions sequestration: Adsorbent modification and activation methods and adsorbent regeneration. *Journal of Environmental Chemical Engineering, 2*(1), 239-259. https://doi.org/10.1016/j.jece.2013.12.019

He, Z. L., Yang, X. E., & Stoffella, P. J. (2005). Trace elements in agroecosystems and impacts on the environment. *Journal of Trace Elements in Medicine and Biology, 19*(2), 125-140. https://doi.org/10.1016/j.jtemb.2005.02.010

Hezarjaribi, M., Bakeri, G., Sillanpää, M., Chaichi, M. J., Akbari, S., & Rahimpour, A. (2021). Novel adsorptive PVC nanofibrous/thiol-functionalized TNT composite UF membranes for effective dynamic removal of heavy metal ions. *Journal of Environmental Management, 284*, 111996. https://doi.org/10.1016/j.jenvman.2021.111996

Hezarjaribi, M., Bakeri, G., Sillanpää, M., Chaichi, M., & Akbari, S. (2020). Novel adsorptive membrane through EMBEDDING thiol-functionalized HYDROUS manganese oxide into PVC ELECTROSPUN NANOFIBER for Dynamic removal OF CU(II) and Ni(II) ions from aqueous solution. *Journal of Water Process Engineering, 37*, 101401. doi:10.1016/j.jwpe.2020.101401

Implen (2021). *UV-vis spectrophotometers: How UV/vis spectrophotometer works*. Implen NanoPhotometers. Retrieved February 4, 2022, from https://www.implen.de/uv-vis-spectrophotometer/

Jaafar, A., Fix-Tailler, A., Mansour, N., Allain, M., Shebaby, W. N., Faour, W. H., Tokajian, S., El-Ghayoury, A., Naoufal, D., Bouchara, J., Larcher, G., & Ibrahim, G. (2020). Synthesis, characterization, antifungal and antibacterial activities evaluation of copper (II), zinc (II) and cadmium (II) chloride and bromide complexes with new (E)-1-(3,4-dimethoxybenzylidene)-4-methylthiosemicarbazone ligand. *Applied Organometallic Chemistry, 34*(12), n/a. https://doi.org/10.1002/aoc.5988

Jaafar, A., Platas-Iglesias, C., & Bilbeisi, R. A. (2021). Thiosemicarbazone modified zeolitic imidazolate framework (TSC-ZIF) for mercury() removal from water. *RSC Advances, 11*(27), 16192-16199. https://doi.org/10.1039/d1ra02025k

Jamshidi Gohari, R., Korminouri, F., Lau, W. J., Ismail, A. F., Matsuura, T., Chowdhury, M. N. K., Halakoo, E., & Jamshidi Gohari, M. S. (2015). A novel super-hydrophilic PSf/HAO nanocomposite ultrafiltration membrane for efficient separation of oil/water emulsion. *Separation and Purification Technology, 150*, 13-20. https://doi.org/10.1016/j.seppur.2015.06.031

Jarup, L. (2003). Hazards of heavy metal contamination. *British Medical Bulletin, 68*(1), 167-182. https://doi.org/10.1093/bmb/ldg032

Khayet, M. S. & Matsuura, T. (2011). *Membrane distillation: Principles and applications*. Elsevier.

Khayyun, T. S., & Mseer, A. H. (2019). Comparison of the experimental results with the langmuir and freundlich models for copper removal on limestone adsorbent. *Applied Water Science, 9*(8), 1-8. https://doi.org/10.1007/s13201-019-1061-2

Kim, H. N., Ren, W. X., Kim, J. S., & Yoon, J. (2012). Fluorescent and colorimetric sensors for detection of lead, cadmium, and mercury ions. *Chemical Society Reviews, 41*(8), 321-3244. https://doi.org/10.1039/c1cs15245a

Kim, J., Kang, T., Kim, H., Shin, H. J., & Oh, S. (2019). Preparation of pva/paa nanofibers containing thiol-modified silica particles by electrospinning as an eco-friendly cu (ii) adsorbent. *Journal of Industrial and Engineering Chemistry, 77*, 273-279. doi:10.1016/j.jiec.2019.04.048

Kostas, I. D., & Steele, B. R. (2020). Thiosemicarbazone complexes of transition metals as catalysts for cross-coupling reactions. *Catalysts, 10*(10), 1-40. https://doi.org/10.3390/catal10101107

Koushkbaghi, S., Zakialamdari, A., Pishnamazi, M., Ramandi, H. F., Aliabadi, M., & Irani, M. (2018). Aminated-Fe3O4 nanoparticles filled Chitosan/pva/pes Dual layers nanofibrous membrane for the removal Of Cr(VI) and Pb(II) ions from aqueous solutions IN Adsorption and membrane processes. *Chemical Engineering Journal, 337*, 169-182. doi:10.1016/j.cej.2017.12.075

Langmuir, I. (1918). the adsorption of gases on plane surfaces of glass, mica and platinum. *Journal of the American Chemical Society, 40*(9), 1361-1403. https://doi.org/10.1021/ja02242a004

Li, M., Zhang, Z., Li, R., Wang, J. J., & Ali, A. (2016). Removal of pb(II) and cd(II) ions from aqueous solution by thiosemicarbazide modified chitosan. *International Journal of Biological Macromolecules, 86*, 876.

Li, Y., Yang, L., Li, X., Miki, T., & Nagasaka, T. (2021). A composite adsorbent of ZnS nanoclusters grown in zeolite NaA synthesized from fly ash with a high mercury ion removal efficiency in solution. *Journal of Hazardous Materials, 411*, 125044-125044. https://doi.org/10.1016/j.jhazmat.2021.125044

Liu, J., Luo, X., Wang, J., Xiao, T., Chen, D., Sheng, G., Yin, M., Lippold, H., Wang, C., & Chen, Y. (2017). Thallium contamination in arable soils and vegetables around a steel plant—A newly-found significant source of tl pollution in south china. *Environmental Pollution (1987)*, 224, 445-453. https://doi.org/10.1016/j.envpol.2017.02.025

Liu, T., Yang, X., Wang, Z., & Yan, X. (2013). Enhanced chitosan beads-supported Fe0-nanoparticles for removal of heavy metals from electroplating wastewater in permeable reactive barriers. *Water Research (Oxford), 47*(17), 6691-6700. https://doi.org/10.1016/j.watres.2013.09.006

Lofrano, G. (2012). *Emerging compounds removal from wastewater: Natural and solar based treatments* (1. Aufl. ed.). Springer.

Marschner, P. (2012). Marschner's mineral nutrition of higher plants (3rd ed.). Academic Press. https://doi.org/10.1016/C2009-0-63043-9

Melnick, J. G., Yurkerwich, K., & Parkin, G. (2010). On the chalcogenophilicity of mercury: Evidence for a strong Hg−Se bond in [TmBut]HgSePh and its relevance to the toxicity of mercury. *Journal of the American Chemical Society, 132*(2), 647-655. https://doi.org/10.1021/ja907523x

Meng, C., Zhikun, W., Qiang, L., Chunling, L., Shuangqing, S., & Songqing, H. (2018). Preparation of amino-functionalized Fe3O4@mSiO2 core-shell magnetic nanoparticles and their application for aqueous Fe3+ removal. *Journal of Hazardous Materials, 341*, 198-206. https://doi.org/10.1016/j.jhazmat.2017.07.062

Metwally, Mohamed & Khalifa, Mohamed & Koketsu, Mamoru. (2012). Thiocarbohydrazides: Synthesis and Reactions. American Journal of Chemistry. 2. 38-51. 10.5923/j.chemistry.20120202.09.

Mohy Eldin, M. S., Tamer, T. M., Abu Saied, M. A., Soliman, E. A., Madi, N. K., Ragab, I., & Fadel, I. (2018). Click grafting of chitosan onto PVC surfaces for biomedical applications. *Advances in Polymer Technology, 37*(1), 38-49. https://doi.org/10.1002/adv.21640

Moulay, S. (2010). Chemical modification of poly(vinyl chloride)-still on the run. *Progress in Polymer Science, 35*(3), 303-331. https://doi.org/10.1016/j.progpolymsci.2009.12.001

National Center for Biotechnology Information (2022). PubChem Compound Summary for CID 2724189, Thiocarbohydrazide. Retrieved February 13, 2022 from https://pubchem.ncbi.nlm.nih.gov/compound/Thiocarbohydrazide.

Ndulue, E. L., Mbajiorgu, C. C., Ugwu, S. N., Ogwo, V., & Ogbu, K. N. (2015). Assessment of land use/cover impacts on runoff and sediment yield using hydrologic models: A Review. *Journal of Ecology and The Natural Environment, 7*(2), 46–55. https://doi.org/10.5897/jene2014.0482

P.N.Sudha, T.E. (2011). Effect of Heavy Metals Copper and Cadmium Exposure on Theantioxidant Properties of The Plant Cleome Gynandra. *The International Journal of Plant, Animal and Environmental Sciences, 2011*; 1:80-7.

Parvate, S., Dixit, P., & Chattopadhyay, S. (2020). Superhydrophobic surfaces: Insights from theory and experiment. *The Journal of Physical Chemistry. B*, 124(8), 1323-1360. https://doi.org/10.1021/acs.jpcb.9b08567

Patrick, L. (2003). Toxic metals and antioxidants: Part II. the role of antioxidants in arsenic and cadmium toxicity. *Alternative Medicine Review, 8*(2), 106.

Pham, L. Q., Uspenskaya, M. V., Olekhnovich, R. O., & Bernal, R. A. O. (2021). A review on electrospun pvc nanofibers: Fabrication, properties, and application. *Fibers, 9*(2), 1-22. https://doi.org/10.3390/fib9020012

Prajapati, N. P., & Patel, H. D. (2019). Novel thiosemicarbazone derivatives and their metal complexes: Recent development. *Synthetic Communications, 49*(21), 2767-2804. https://doi.org/10.1080/00397911.2019.1649432

Rafati Rahimzadeh, M., Rafati Rahimzadeh, M., Kazemi, S., & Moghadamnia, A. (2017). Cadmium toxicity and treatment: An update. *Caspian Journal of Internal Medicine, 8*(3), 135-145. https://doi.org/10.22088/cjim.8.3.135

Ritger, A. L., Curtis, A. N., & Chen, C. Y. (2018). Bioaccumulation of mercury and other metal contaminants in invasive lionfish (pterois volitans/miles) from curaçao. *Marine Pollution Bulletin, 131*(Pt A), 38-44. https://doi.org/10.1016/j.marpolbul.2018.03.035

RSC (2022). *Silver - element information, properties and uses.* Retrieved July 2, 2022, from https://www.rsc.org/periodic-table/element/47/silver#:~:text=It%20is%20used%20for%20jewellery,alloys%2C%20electrical%20contacts%20and%20batteries.

Sigel, A., Sigel, H., & O., S. R. (2017). *Lead: Its effects on environment and health*. Berlin: De Gruyter.

Siyal, A. A., Shamsuddin, M. R., Khan, M. I., Rabat, N. E., Zulfiqar, M., Man, Z., . . . Azizli, K. A. (2018). A review on geopolymers as emerging materials for the

adsorption of heavy metals and dyes. *Journal of Environmental Management, 224*, 327-339. doi:10.1016/j.jenvman.2018.07.046

Suja, P. S., Reshmi, C. R., Sagitha, P., & Sujith, A. (2017). Electrospun Nanofibrous membranes for water purification. Polymer Reviews, 57(3), 467-504. doi:10.1080/15583724.2017.1309664

Tchobanoglous, G., Burton, Franklin L. (Franklin Louis), Stensel, H. D., & Metcalf & Eddy. (2003). *Wastewater engineering: Treatment and reuse* (4th ed.). McGraw Hill.

Tchounwou, P. B., Yedjou, C. G., Patlolla, A. K., & Sutton, D. J. (2012). Heavy metal toxicity and the environment. *Molecular, clinical and environmental toxicology* (pp. 133-164). Springer Basel. https://doi.org/10.1007/978-3-7643-8340-4_6

U. S. Geological Survey. (2012). in *Historical statistics for mineral and material commodities in the United States*, Vol. 140, pp. 36–37.

United States Environmental Protection Agency (US-EPA) (2012). 2012 Edition of the Drinking Water Standards and Health Advisories. Washington, DC, EPA 822-S-12-001. Available at: https://www3.epa.gov/region9/water/drinking/files/dwshat-v09.pdf.

Wang, G., Zhang, S., Xu, X., Li, T., Li, Y., Deng, O., & Gong, G. (2014). Efficiency of nanoscale zero-valent iron on the enhanced low molecular weight organic acid removal pb from contaminated soil. *Chemosphere (Oxford), 117*(1), 617-624. https://doi.org/10.1016/j.chemosphere.2014.09.081

Wang, H., Yang, X., Wang, M., Hu, M., Xu, X., Yan, A., Hao, Q., Li, H., & Sun, H. (2020). Atomic differentiation of silver binding preference in protein targets: Escherichia coli malate dehydrogenase as a paradigm. *Chemical Science (Cambridge), 11*(43), 11714-11719. https://doi.org/10.1039/d0sc04151c

Wang, H., Zhou, A., Peng, F., Yu, H., & Yang, J. (2007). Mechanism study on adsorption of acidified multiwalled carbon nanotubes to pb(II). *Journal of Colloid and Interface Science, 316*(2), 277.

Wang, T., Liu, W., Xu, N., & Ni, J. (2013). Adsorption and desorption of cd(II) onto titanate nanotubes and efficient regeneration of tubular structures. *Journal of Hazardous Materials, 250-251*, 379-386. https://doi.org/10.1016/j.jhazmat.2013.02.016

World Health Organisation (WHO) (2011). Guidelines for Drinking WaterQuality, 4th ed., vol. 1. World Health Organization, Geneva. NLMclassification: WA 675. ISBN 978 92 4 154815 1. Available at: http://www.who.int/water_sanitation_health/publications/2011/9789241548151_toc.pdf

WQA. (2004). *Recognized Treatment Techniques for Meeting Drinking Water Regulations for The Reduction of Silver from Drinking Water Supplies Using Point-of-Use/Point-of-Entry Devices And Systems*.

Wu, H., Li, T., Liu, B., Chen, C., Wang, S., & Crittenden, J. C. (2018). Blended PVC/PVC-g-PEGMA ultrafiltration membranes with enhanced performance and antifouling properties. *Applied Surface Science*, 455, 987-996. https://doi.org/10.1016/j.apsusc.2018.06.056

Yang, D., Li, L., Chen, B., Shi, S., Nie, J., & Ma, G. (2019). Functionalized chitosan electrospun nanofiber membranes for heavy-metal removal. *Polymer, 163*, 74-85. doi:10.1016/j.polymer.2018.12.046

Youness, F. (2021). Preparation and Characterization of Triethylenetetramine Modified Electrospun Membranes (TETA - PVC) and Their Adsorption Behavior in Removing Lead(II) From Water [Master's Thesis, American University of Beirut]. AUB ScholarWorks. https://scholarworks.aub.edu.lb/bitstream/handle/10938/23027/YounessFatima_2021.pdf?sequence=1&isAllowed=y

Zang, L., Lin, R., Dou, T., Lu wang, L. W., Ma, J., & Sun, L. (2019). Electrospun superhydrophilic membranes for effective removal OF Pb(ii) from water. *Nanoscale Advances, 1*(1), 389-394. doi:10.1039/c8na00044a

Zhao, J., & He, M. (2014). Theoretical study of heavy metal cd, cu, hg, and ni(II) adsorption on the kaolinite(001) surface. Applied Surface Science, 317, 718-723. https://doi.org/10.1016/j.apsusc.2014.08.162

Zhu, F., Zheng, Y., Zhang, B., & Dai, Y. (2021). A critical review on the electrospun nanofibrous membranes for the adsorption of heavy metals in water treatment. *Journal of Hazardous Materials, 401*, 123608. doi:10.1016/j.jhazmat.2020.123608

Zhuang, P., McBride, M. B., Xia, H., Li, N., & Li, Z. (2009). Health risk from heavy metals via consumption of food crops in the vicinity of dabaoshan mine, south china. *The Science of the Total Environment, 407*(5), 1551-1561. https://doi.org/10.1016/j.scitotenv.2008.10.061